Development of mathematical model to predict ship maneuvering

NORDCO Limited

Contractor Report (National Research Council of Canada. Institute for Marine Dynamics); no. CR-1989-28, 1989

National Research Council Canada
Conseil national de recherches Canada
Institute for Ocean Technology
Institut des technologies océaniques

CR-1989-28

Contractor Report

Development of Mathematical Model to Predict Ship Maneuvering, Part I: Formulations and Verifications

NORDCO Ltd.

March 1989

Canada

DEVELOPMENT OF MATHEMATICAL MODEL TO PREDICT SHIP MANEUVERING

Part I - Formulations and Verifications

Submitted to: NRC, Institute for Marine Dynamics
Submitted by: NORDCO Limited
NORDCO Ref.: 44-88G-3
Date: March 31, 1989

DOCUMENTATION PAGE

REPORT NUMBER	NRC REPORT NUMBER	DATE
CR-1989-28	-	March 1989

REPORT SECURITY CLASSIFICATION	DISTRIBUTION
Unclassified	Unlimited

TITLE

DEVELOPMENT OF MATHEMATICAL MODEL TO PREDICT SHIP MANEUVERING
PART I - FORMULATIONS AND VERIFICATIONS

AUTHOR(S)
NORDCO Limited

CORPORATE AUTHOR(S)/PERFORMING AGENCY(S)

NORDCO Limited

PUBLICATION

-

SPONSORING AGENCY(S)

Institute for Marine Dynamics
National Research Council Canada

IMD PROJECT NO.	NRC FILE NO.
052	7816

KEY WORDS:	PAGES	FIGS.	TABLES
restricted water, wind effect, current effect, bow propeller	ii, 29	27	6

SUMMARY: This report describes the mathematical modelling of the effects of wind, current and bow thrusters on maneuvering and of maneuvering in shallow water and narrow channels.

ADDRESS: National Research Council
Institute for Marine Dynamics
P.O. Box 12093, Stn 'A'
St. John's, NF
A1B 3T5

TABLE OF CONTENTS

		Page
1.0	**INTRODUCTION**	1
2.0	**MATHEMATICAL FORMULATIONS**	2
2.1	Equations of Motion	2
2.2	Engine Model	2
2.3	Shallow Water Effects	3
2.3.1	Assumptions and Limitations	4
2.3.2	Hydrodynamic Derivatives	4
2.3.3	Surge Equation - Resistance and Propeller Thrust	6
2.4	Rudder Forces and Moments	8
2.5	Bank and Channel Effects	9
2.6	Bow Thruster	10
2.7	Wind Effects	11
2.8	Current Effects	12
2.9	Environmental Data Base	15
3.0	**MANEUVERING MODEL IMPLEMENTATION**	15
4.0	**VERIFICATION**	15
4.1	Engine Model	16
4.2	Shallow Water	16
4.2.1	Shallow Water Effects on Resistance and Propeller Thruster	16
4.2.2	Shallow Water Effects on Maneuverability	17
4.3	Bank and Channel	18
4.4	Bow Thruster	18
4.5	Wind	18
4.6	Current	19
5.0	**CONCLUSIONS**	
6.0	**RECOMMENDATIONS**	
7.0	**REFERENCES**	
8.0	**BIBLIOGRAPHY**	
LIST OF TABLES		
LIST OF FIGURES		
NOMENCLATURE		

DEVELOPMENT OF MATHEMATICAL MODEL TO PREDICT SHIP MANEUVERING

1.0 INTRODUCTION

This report is an extension of the work presented in the reports "Mathematical Simulation of Ship Maneuvering" and "Mathematical Simulation of Ship Maneuvering, Part 2 - Program Verification and Study of Hull, Propeller, and Rudder Interactions" [1]. In the previous studies, a hydrodynamic derivative type mathematical maneuvering simulation model was developed and implemented based on Inoue's formulations and the capability of the model to simulate ship maneuvering behaviour in open water without external influences was demonstrated. In order to increase its versatility, further development to include external influences (current, wind and bow thruster) and restricted water effects (shallow water and channel) into the maneuvering simulation model is planned. In addition, previous studies also indicated the need of a user editable hydrodynamic derivative file whereby tuning of the hydrodynamic derivatives to better match the maneuvering characteristics of particular ships can be accomplished, and the need of a reference source of model-scale and full-scale maneuvering test results with the corresponding ship particulars whereby the maneuvering simulation model can be verified.

The purpose of this report is to record the progress made regarding to the needs identified previously; special emphasis is placed on the documentation of the mathematical modellings and software implementation of the external influences and restricted water effects since they are the thrust of the present study. However, the mathematical modellings of the additional features (external influences and restricted water effects) are limited to those published in the open literature and no attempt is made to derive them theoretically since this is beyond the scope of the present project. The software implementations is developed with maximum flexibility to account for the arbitrary situations foreseeable.

This report is divided into three parts. Part I describes the formulations used in the mathematical modelling of the additional features and their derivations from the literature. It also discusses the verifications of their implementations into the maneuvering simulation model with reference to the reference source mentioned previously. Since Part I is the main part of the report, it also includes the conclusions and recommendations for future study regarding the present project. Part II describes the software implementations of the additional features and the program structure of the maneuvering simulation model; it also contains the source code of the main part of the maneuvering simulation programs. Part III describes the usage of the maneuvering simulation model program including direction for editting the hydrodynamic derivative file for tuning, and it also contains the source code of the remaining programs not included in Part II.

2.0 MATHEMATICAL FORMULATIONS

2.1 Equations of Motion

The equations of motion of the maneuvering simulation model are written with respect to a moving coordinate system fixed on the center of gravity of the ship,

Surge: $m(\dot{u}-vr) = X_H+X_P+X_R+X_O$ (2.1)

Sway: $m(\dot{v}+ur) = Y_H+Y_R+Y_O$ (2.2)

Yaw: $I_{zz}\dot{r} = N_H+Y_{HO}x + N_R+N_O$ (2.3)

Roll: $I_{xx}\ddot{\theta} = K_H-Y_Hz_H+K_R+K_O$ (2.4)

The terms with subscript H represent the hydrodynamic forces and moments induced by the ship's motion; the term with subscript P represents the force induced by the propeller; and the terms with subscript R represent those induced by the rudder. The descriptions and calculations of these forces and moments were documented in detail in the previous report [1]. The terms with subscript O represent other external forces and moments due to bank and channel, bow thruster and wind. The formulations of the external forces and the incorporation of current, engine model and shallow water effects are presented in the following sections.

2.2 Engine Model

In order to account for the effects of power plant on ship's maneuvering characteristics, an engine model equation is incorporated into the model. It is written as,

$$I_{pp}\dot{n}(2\pi/60) = Q_E - Q_p \quad (2.5)$$

where I_{pp}= moment of inertia of propeller-shaft system

Q_p= propeller torque

Q_E= torque delivered by power plant

n = time rate of change of propeller rpm

The moment of inertia of the propeller is approximated based on the propeller diameter,

$$I_{pp} = 20\,D_p^5 \ \text{kg-m}^2$$

and the propeller torque Q_p dispensed at the propeller is determined from the torque coefficient K_Q versus advance coefficient Jp table of the Wageningen B-series propeller of

similar geometry [2]; the procedure is identical to those used to determine the thrust coefficient K_T in the previous report [1]. Q_E represents the power plant torque characteristics. Two types of power plant are modelled - steam turbine and slow speed diesel.

For a steam turbine,

$$Q_E = \frac{60}{2\pi} \frac{SHP}{n_c} = \frac{60}{2\pi} \frac{SHP}{n_{cp} \times R_{GEAR}} \qquad (2.6)$$

where SHP = engine shaft horsepower in N-m/sec
n_c = command engine rpm
n_{cp} = equivalent command propeller rpm
R_{GEAR} = reduction gear ratio

and for a slow speed diesel engine,

$$Q_E = Q_{p@u_E \text{ w.r.t.n.}_c}, \quad Q_E \leq Q_{EMax} \qquad (2.7)$$

where u_E = equilibrium straight ahead speed corresponds to a propeller rpm of n_{cp}

Q_{Emax} = maximum engine torque available

In the engine model calculation two propeller rpms are used, n and n_{cp}. n_{cp} is the actual propeller rpm commanded at helm and n is the instantaneous rpm of the propeller. When a ship is maneuvering, its actual propeller rpm is usually different from the one commanded; the difference between n and n_{cp} is dependent on the stage and type of maneuver the ship is undergoing and the torque characteristics of the power plant. The equilibrium speed u_E is determined by equating the resistance X(u) and propeller thrust X_p (corresponding to n_{cp}) in the surge equation. X(u) is expressed as a function of ship speed in the resistance table and X_p is calculated from K_T which is determined from the propeller thrust table. At equilibrium speed,

$$X(u_E) = X_p(J_{pE}) \qquad (2.8)$$

where $J_{pE} = 60\, u_E(1-w_{po})$ = equilibrium advance coefficient

2.3 Shallow Water Effects

In shallow water, the maneuvering characteristics of the ship change according to the water depth to draft ratio h/T. As the depth decreases, water can no longer pass unrestrictedly underneath the ship due to the contriction between its keel and the sea bottom. This increases the flow around the side of the ship and consequently changing the hydrodynamic forces exerted on the ship.

According to Hooft [3], the longitudinal forces acting on the ship are influenced by water depth at h/T ratio of less than 3.5, the lateral forces are influenced at h/T ratio of less than 2.5, and at h/T less than 1.5 the ship's maneuvering characteristics are changed appreciably from those of deep water.

In order to account for the influences of the shallow water on the ship's maneuvering characteristics, the calculation of the hydrodynamic derivatives, longitudinal resistance, propeller thrust, engine model, rudder forces and moments are modified in the model.

2.3.1 Assumptions and Limitations

The following assumptions and limitations are imposed on the modifications for shallow water effects;

1. When h/T 3.5, the ship is at shallow water;

2. The ship speed is below the critical speed, i.e. u /gh;

3. The formulations are based on theoretical considerations and model experiments. They cannot be considered as theoretically rigorous but may be considered as good engineering solutions of a confused and complicated problem;

4. Constant propulsive power that Q_E is a function of n_c and independent of water depth; and

5. The propeller torque Q_P is determined from the deep water K_Q value with J_P calculated using u and n in shallow water [4].

2.3.2 Hydrodynamic Derivatives

A practical way to determine added mass and velocity coefficients in shallow water is to find the ratio of their shallow water to deep water values as function of h/T so that

$$f(h/T) = \frac{\text{Hydrodynamic Derivative at Water Depth h}}{\text{Hydrodynamic Derivative at Deep Water}}$$

Hirano [5] and Sheng [6] published formulae of f(h/T) for the linear hydrodynamic derivatives. Hirano's results were derived using experimental data and low aspect ratio wing theory by assuming the hull as an airfoil. Sheng's results were derived using strip theory by assuming the ship as a parabolic beam with elliptical section. Sheng's formulae were verified with the experimental results of Fujino [7] and used by Clarke [8].

Therefore, Sheng's formulae are adapted in the model for the added mass coefficients and linear velocity coefficients:

$$\frac{m_y}{m_{y\infty}} = K_0 + 2/3\ K_1\ B/T + 8/15\ K_2\ (B/T)^2 - K^3 \qquad (2.10)$$

$$\frac{m_v}{m_{v\infty}} = K_0 + 2/5\ K_1\ B/T + 24/105\ K_2\ (B/T)^2 \qquad (2.11)$$

$$\frac{Y'_{uv}}{Y'_{uv\infty}} = K_0 + K_1\ B/T + K_2\ (B/T)^2 \qquad (2.12)$$

$$\frac{Y'_{ur}}{Y'_{ur\infty}} = K_3 \qquad (2.13)$$

$$\frac{N'_{uv}}{N'_{uv\infty}} = K_3 \qquad (2.14)$$

$$\frac{N'_{ur}}{N'_{ur\infty}} = K_0 + 1/2\ K_1\ B/T + 1/3\ K_2\ (B/T)^2 \qquad (2.15)$$

where $K_0 = 1 + \frac{0.0775}{(h/T-1)^2} - \frac{0.011}{(h/T-1)^3}$

$K_1 = \frac{0.0643}{(h/T-1)} + \frac{0.072}{(h/T-1)^2} - \frac{0.0113}{(h/T-1)^3}$

$K_2 = \frac{0.0342}{(h/T-1)}$

The change in surge added mass in shallow water is less than 10% of its deep water value and it is assumed to be unchanged in the model. Similarly, the roll added mass is also assumed constant regardless of the water depth.

No formula for the non-linear velocity coefficients $Y'_{v\,r}$, $Y'_{r\,r}$, N'_{vvr}, N'_{vrr} and $N'_{r\,r}$ is found from the open literature expect for the coefficient Y'_{vv}. Zhu [9] reported,

$$Y'_{vv} = \int_{-1/2}^{1/2} f(T/h, x')\, C_D(x') \left|v' + x'_M r'\right| (v' + x'_M r')\, dx' \qquad (2.16)$$

where $f(T/h,x')$ = function of draft to depth ratio along the ship's length

$C_D(x')$ = sectional drag coefficient in shallow water

The prime denotes non-dimensional length, velocity and yaw rate. According to eq. 2.16, the sectional drag coefficients along the ship in shallow water must be known before Y'_{vv} can be calculated. However, the ship's sectional drag ceofficients at different depths are not generally known; therefore, the applicability of Zhu's formula is limited.

Fujino [10], Yumuro [11] and Kijima [12] conducted model test to determine the variation of non-linear hydrodynamic derivatives with water depth. Based on these findings, a general variation of f(T/h), the shallow water to deep water value ratio, to T/h can be constructed, Figure 2.1. From Figure 2.1, at deep water where the T/h ratio equals zero, it is obvious that f(o) is one. The ratio does not increase significantly until T/h is more than 0.29 (h/T 3.5), and it doubles its value when T/h reaches 0.4 (h/T = 2.5). A maximum value ranging from 3 to 5* is reached when T/h is around 0.8 (h/T=1.25), and then it decreases as T/h increases.

Due to the lack of information, the f(T/h) versus T/h curve proposed in Figure 2.1 is curve fitted in the model to calculate the non-linear hydrodynamic derivatives in shallow water from their deep water values. However, if the actual variations of the non-linear hydrodynamic derivatives are known, they can be incorporated using the same curve fitting routine.

2.3.3 Surge Equation - Resistance and Propeller Thrust

When a ship enters into shallow water, its speed will decrease whilst the longitudinal resistance and propeller thrust will increase. In order to calculate the surge velocity, the values of resistance X(u) and propeller thrust X_p in shallow water must be known explicitly.

From the previous report [1], the values of X(u) and X_p in deep water are determined from the resistance versus speed table and thrust coefficient versus advanced coefficient table tabulated in the ship description file. However, it will be impractical to tabulate the same tables for different water depths. Therefore, the shallow water resistance and propeller thrust are calculated using Schwanecke's formulae [13],

$$X(u_h) = X(u_\infty)\left(\frac{u_h}{u_\infty}\right)^2 \text{EXP}\,(0.11\, F_{nh}^2\ B/h-T) \qquad (2.17)$$

$$(X_p)_h = (X_p)_\infty\left(\frac{u_h}{u_\infty}\right)^2 \text{EXP}\,(0.30\, F_{nh}^3\ B/h-T) \qquad (2.18)$$

* depending on the hydrodynamic derivative

where F_{nh} = shallow water Froude number = $u_h/\sqrt{gh}$

The subscript h and ∞ denote shallow and deep water, respectively.

Since the resistance and propeller thrust in shallow water in eq. 2.17 and 2.18 are determined from their deep water values at the corresponding u_∞, a correlation between u_∞ and u_h is required.

The shallow water velocity u_h is calculated from u_∞ at the same propeller rpm using Schlichting's hypothesis [14]. Schlichting separated the total resistance in shallow water into wave-making resistance and resistance due to viscous flow around the hull. He further assumed that the wave-making resistance in shallow water is identical to those in deep water when the same wave pattern is generated. Using linear wave theory, he related u_∞ to an intermediate velocity u_I in shallow water where the wave-making resistances are identical, and u_I is expressed as a function of $u_\infty/\sqrt{gh}$. Then using model test results, he examined the velocity decrease due to viscosity in shallow water and related u_h with u_I as a function of the blockage parameter $\sqrt{A_x}/h$, where A_x is the maximum cross-sectional area of the hull. Figure 2.2 shows the u_I versus $u_\infty/\sqrt{gh}$ and Figure 2.3 shows the u_h versus $\sqrt{A_x}/h$ curves, both of these curves and their inverse are incorporated into the maneuvering model to evaluate u_h from u_∞ and vice versa.

The procedure of using Schlichting's hypothesis and Schwanecke's formulae in the surge equation (when a ship enters shallow water of depth h, with speed u_∞, and propeller rpm n) is as follows:

1. Calculate u_h from u_∞ and h using Schlichting's hypothesis;

2. Calculate $X(u_h)$ from u_h, u_∞, and $X(u_\infty)$ using eq. 2.17;

3. Calculate $(X_p)_h$ from u_h, u_∞, and $(X_p)_\infty$ at u_∞ and n using eq. 2.18;

4. Calculate $(u_h)_{NEW}$ using the surge equation;

5. Calculate n_{NEW} using the engine model equation with assumption 4 and 5;

6. Calculate $(u_\infty)_{NEW}$ corresponds to $(u_h)_{NEW}$ using the inverse of Schlichting's hypothesis; and

7. $u_h = (u_h)_{NEW}$, $u_\infty = (u_\infty)_{NEW}$ and $n = n_{NEW}$, go to Step 2.

Step 2 to 7 are repeated as long as the ship is in shallow water.

2.4 Rudder Forces and Moments

Fujino [7,15] claimed that water depth has little effect on the rudder force due to two compensating effects:

1. the effectiveness of the rudder diminishes due to increase in flow separation at the stern; and

2. the effectiveness of the rudder increases due to a stronger propeller slipstream resulting from the reduced speed due to increase resistance in shallow water.

Similar observations are reported by Kose [16] and Hooft [3] that shallow water effects on the rudder are small. However, Yumuro [17] and Hirano [18] suggested that the rudder-hull interaction force and the flow-rectifying effect related to the rudder inflow angle are affected by water depth. Therefore, the rudder induced force and moment expressions in the previous model [1] are modified,

$$Y_R = -(1 + a_H) F_N \cos \delta \qquad (2.19)$$

$$N_R = (x_R + a_H x_H) F_N \cos \delta \qquad (2.20)$$

$$K_R = (1 + a_H) z_H F_N \cos \delta \qquad (2.21)$$

where x_H = point of application of rudder induced interaction force on ship hull = f(T/h)

x_R = horizontal distance between center of gravity and rudder

a_H = ratio of rudder induced hull force to rudder force = f(T/h)

The parameters a_H, x_H and the flow-rectifying parameter γ change with water depth as,

$$a_H = a_{H\infty} + C_1 (T/h) + C_2 (T/h)^2 = a_{H\infty} + \Delta a_H \qquad (2.22)$$

$$x_H = x_{H\infty} + C_3 (T/h) + C_4 (T/h)^2 \qquad (2.23)$$

$$\gamma = [0.332 (T/h) + 1] \gamma_\infty \qquad (2.24)$$

where $a_{H\infty} = 0.627\ C_B - 0.153$

$x_{H\infty} = 0.5\ L_{pp}$

The subscript ∞ denotes deep water value and the coefficients C_1 to C_4 in eq. 2.22 and 2.23 are determined by cubic splines curve fitting technique using Hirano's data [5], listed in Table 2.1 and 2.2.

2.5 Bank and Channel Effects

When a ship is travelling off the centerline of a channel, it experiences a suction force and a bow-out moment to the near bank due to flow asymmetry around the hull, Figure 2.4. The bank force is highly non-linear and varies almost inversely with the ship-to-bank distance [19]. Although the hydrodynamic coefficients are also affected, the maneuvering model only considers the bank force and moment since they are the primary influences of the channel [7]. The effects on the hydrodynamic derivatives due to finite depth described in the previous section are imposed in the channel; however, the cross-coupling between the shallow water effects and channel effects is ignored in the model [20].

Norrbin [21] and Eda [22] published empirical formulae for the bank force and moment but they pertained to two specific ships only. On the other hand, Schoenherr [23] derived simple non-dimensionalized design charts for estimating the bank force and moment on full-form merchant ship hull. These charts are expressed as functions of channel depth to draft ratio h/T, channel width to beam ratio W/B, and off-centerline distance to beam ratio Y_{CL}/B, Figure 2.4.

Since Schoenherr's charts are the only source identified for bank force and moment estimation, it is adapted into the model as,

$$Y_{CHANNEL} = C_F \times \alpha \times 1/2 \rho L T u^2 \qquad (2.25)$$

$$N_{CHANNEL} = Y_{CHANNEL} \times L \times x_C \qquad (2.26)$$

where C_F = channel force coefficient at h/T = 1.40

α = depth correction factor
= (C_F at given h/T)/(C_F at h/T = 1.40)

x_c = location of the center of lateral pressure

The coefficient C_F is determined from Figure 2.5 as a function of Y_{CL}/B and W/B. The parameters α and x_c are determined from Figure 2.6 and 2.7 as a function of h/T, respectively. The off-centerline distance, Y_{CL}, is measured at L/4 fore of

midship because this will generate a bank force and moment when the ship is travelling with a drift angle along the centerline, Figure 2.8. This is a more realistic representation than measuring Y_{CL} at midship where the ship will experience no bank effect in that situation.

2.6 Bow Thruster

The effects of bow thruster as a maneuvering aid are modelled by a side force and an external moment it generates. In addition, the decrease in effectiveness of the bow thruster due to the increase of ship speed is also incorporated into the model [24].

The side force produced by the thruster is calculated using the rated power, thruster impeller diameter and a merit coefficient which was determined experimentally based on thruster type and its pitch/diameter ratio [25] in Figure 2.9,

$$Y_{THRUSTER} = (shp \sqrt{\frac{\rho \pi D_B^2}{4}} \; C)^{2/3} \qquad (2.27)$$

where shp = thruster shaft horsepower in N-m/sec
D_B = impeller diameter
C = merit coefficient according to Figure 2.9

The turning moment generated is calculated using,

$$N_{THRUSTER} = Y_{THRUSTER} \times X_T \qquad (2.28)$$

where x_T = distance from bow thruster to midship

The ship speed effects on the effectiveness of the bow thruster are accounted for by the body force and body moment coefficients,

$$Y_{THRUSTER} = K_F \times Y_{THRUSTER_{@\,U-0}} \qquad (2.29)$$

$$N_{THRUSTER} = K_M \times N_{THRUSTER_{@\,U-0}} \qquad (2.30)$$

where K_F = body force coefficient
K_M = body moment coefficient

K_F and K_M are expressed as a function of the ship speed to jet velocity ratio, u/u_j [26] and Figure 2.10 shows the relationship of K_F and K_M with u/u_j ratio used in the model. The jet velocity u_j is the momentum mean jet velocity based on the static thrust,

$$u_j = (Y_{THRUSTER} / \rho A_B)^{1/2} \quad (2.31)$$

where A_B = duct cross-sectional area = $\pi D^2_B/4$

and

$$U = (u^2 + v^2)^{1/2} \quad (2.32)$$

2.7 Wind Effects

The wind induced forces and moments on the ship are estimated by the formulae published by Isherwood [27], which were based on 49 sets of wind tunnel test data conducted at different test establishments. The data covered a wide range of ships, and the formulae are valid for estimating the components of wind induced force and yaw moment on any merchant ship form with wind from any direction. Isherwood's formulae are adopted by Wilson [28] and Hirano [29] in their maneuvering simulation models.

The wind induced forces and moments are calculated from the following formulae:

$$X_{WIND} = 1/2\ \rho_{AIR}\ u_W^2 A_T C_X \quad (2.33)$$

$$Y_{WIND} = 1/2\ \rho_{AIR}\ u_W^2 A_L C_Y \quad (2.34)$$

$$N_{WIND} = 1/2\ \rho_{AIR}\ u_W^2 A_L L_{OA} C_N \quad (2.35)$$

where C_X = fore and aft force coefficient

$$= A_0 + A_1 \frac{2A_L}{L_{OA}^2} + A_2 \frac{2A_T}{B^2} + A_3 \frac{L_{OA}}{B} + A_4 \frac{S}{L_{OA}} + A_5 \frac{C_L}{L_{OA}} + A_6 M$$

C_Y = lateral force coefficient

$$= B_0 + B_1 \frac{2A_L}{L_{OA}^2} + B_2 \frac{2A_T}{B^2} + B_3 \frac{L_{OA}}{B} + B_4 \frac{S}{L_{OA}} + B_5 \frac{C_L}{L_{OA}} + B_6 \frac{A_{SS}}{A_L}$$

C_N = yawing moment coefficient

$$= C_0 + C_1 \frac{2A_L}{L_{OA}^2} + C_2 \frac{2A_T}{B^2} + C_3 \frac{L_{OA}}{B} + C_4 \frac{S}{L_{OA}} + C_5 \frac{C_L}{L_{OA}}$$

ρ_{AIR} = density of air

U^2_W = relative wind velocity

A_T = transverse projected area

A_L = lateral projected area

L_{OA} = length overall

A_{SS} = lateral projected area of superstructure

S = length of perimeter of lateral projection of model excluding waterline and slender bodies such as masts and ventilators

C_L = distance from bow to the lateral-projected-area's centroid

M = number of distinct groups of masts or kingposts seen in lateral projection; kingposts close against the bridge front are not included

The aerodynamic coefficients A_0 to A_6, B_0 to B_6 and C_0 to C_5 are tabulated in Table 2.3, 2.4 and 2.5 with respect to the relative wind angle γ_{WIND} measured off the bow. In Table 2.3 to 2.5, γ_{WIND} ranges 0° to 180° in increments of 10° and linear interpolation is used to find the aerodynamic coefficients for the in between γ_{WIND} values.

2.8 Current Effects

There are two approaches to incorporate the current effects into the maneuvering model [30]. One approach is to form two acceleration components of the current in the coordinate system moving with the ship. The two acceleration components are:

$$\ddot{x}_{CURRENT} = \frac{Du_C}{Dt} \cos\psi + \frac{Dv_C}{Dt} \sin\psi \qquad (2.36)$$

$$\ddot{y}_{CURRENT} = -\frac{Du_C}{Dt} \sin\psi + \frac{Dv_C}{Dt} \cos\psi \qquad (2.37)$$

where u_c = the x-component of current velocity over ground (with respect to the earth fixed coordinate)

v_c = the y-component of current velocity over ground

$\frac{D}{Dt}$ = the total derivative = $\frac{\partial}{\partial t} + u_e \frac{\partial}{\partial t} + v_e \frac{\partial}{\partial t}$

u_e = x-component of ship speed over ground
= $u\cos\phi - v\sin\phi + u_c$

v_e = y-component of ship speed over ground
= $u\sin\phi + v\cos\phi + v_c$

Assuming that the current variation occurs over a distance larger than the length of the ship, the current forces exerted on the center of gravity of the ship are written as,

$$X_{CURRENT} = - m \ddot{x}_{CURRENT} \quad (2.38)$$

$$Y_{CURRENT} = - m \ddot{y}_{CURRENT} \quad (2.39)$$

An alternative approach, adapted in the model, is to express the ship speed (as seen from the earth fixed coordinate system) as sum of the speed relative to water plus the velocity of current. Thus,

$$u = u_S + u_C \quad (2.40)$$

$$v = v_S + v_C \quad (2.41)$$

$$r = r_S + r_C \quad (2.42)$$

The subscript s and c denote velocity relative to water and velocity of current, respectively. The equations of motion, eq. 2.1 to 2.4, are rewritten as,

$$m[(\dot{u}_S + \dot{u}_C) - (v_S + v_C)(r_S + r_C)] = (X_H + X_P + X_R)_{@u_S} + X_O \quad (2.43)$$

$$m[(\dot{v}_S + \dot{v}_C) + (u_S + u_C)(r_S + r_C)] = (Y_H + Y_R)_{@u_S} + Y_O \quad (2.44)$$

$$I_{zz}(\dot{r}_S + \dot{r}_C) = (N_H + Y_{HO} x_M + N_R)_{@u_s} + N \tag{2.45}$$

$$I_{xx}\dot{\Phi} = (K_H - Y_H z_H + K_R)_{@u_s} + K_O \tag{2.46}$$

$$I_{pp}\dot{n}(2\pi/60) = Q_E - Q_{P@u_s} \tag{2.47}$$

The force and moment terms in bracket on the right hand side of the equations of motion, eq. 2.42 to 2.45, are not affected by the current, but they are determined by the relative velocity between the ship and water.

The ship's trajectory is determined by integrating its velocity over ground,

$$\dot{x}_e = (u_S + u_C)\cos\psi - (v_S + v_C)\sin\psi \tag{2.48}$$

$$\dot{y}_e = (u_S + u_C)\sin\psi + (v_S + v_C)\cos\psi \tag{2.49}$$

$$\dot{\psi}_e = r_S + r_C \tag{2.50}$$

$$\dot{\Phi}_e = \dot{\Phi} \tag{2.51}$$

The current velocity is defined by four check points along the ship's length, Figure 2.11. In components form,

$$u_{ci} = u_{ci}\cos(\theta_{ci} - \psi), \; i=1 \text{ to } 4 \tag{2.52}$$

$$v_{ci} = u_{ci}\sin(\theta_{ci} - \psi), \; i=1 \text{ to } 4 \tag{2.53}$$

where U_{ci} and θ_{ci} are the magnitude and direction of current at position x_{ei} and y_{ei}, respectively.

$$u_C = \frac{1}{4} \sum_{i=1}^{4} u_{ci} \tag{2.54}$$

$$v_C = \frac{1}{4} \sum_{i=1}^{4} v_{ci} \tag{2.55}$$

$$r_C = \frac{1}{4} \left[\frac{v_{C1}}{l_1} + \frac{v_{C2}}{l_2} - \left(\frac{v_{C3}}{l_3} + \frac{v_{C4}}{l_4} \right) \right] \tag{2.56}$$

where l_i is the distance of check point i form midship as shown in Figure 2.11.

The purpose of using four check points is to simulate the current induced yaw due to non-uniform current along the ship's length.

2.9 Environmental Data Base

The current, wind or shallow water effects are function of the ship position. In order to determine these effects, the magnitudes and directions of the current and wind, and the water depth must be known over the entire maneuvering area. However, environmental data on current, wind and depth in such detail are usually scarce. Therefore, a surface fitting routine using thin plate splines technique [31] is developed to calculate the local environmental conditions at the ship position from the environmental data available for the area of interest.

3.0 MANEUVERING MODEL IMPLEMENTATION

The implementations of the different effects described in the previous chapter are documented in Part II of the Development of Mathematical Model to Predict Ship Maneuvering Report.

4.0 VERIFICATION

Two aspects are involved in the verification process regarding the maneuvering simulation model; one concerns the mathematical modellings and the other concerns the coding of the computer program. Since the mathematical modellings of the external influences are taken from recognized sources, the verification process is focused on the accuracy of the coding. With the engine model, shallow water, bank and channel, bow thruster, wind and current effects incorporated, the maneuvering simulation model program has become substantially more complex than the original and extensive testing is required to ensure the model is implemented correctly.

In the verification process, the simulated results are compared with those obtained from sea trial and model test when information is available. An attempt is made to establish, from open literature, a reference source of model-scale and full-scale maneuvering test results and the corresponding ship particulars for verification of the model; however, as the previous reports [1] have indicated, data useable for comparison are scarce. Published data often lack the pertinent information required by the maneuvering simulation model in order to produce comparable results. Nevertheless, the information collected for the reference source is compiled in the bibliography section of this report. The bibliography is divided into six topics: channel, hydrodynamic coefficients, maneuvering data, propulsion and resistance, shallow water and thruster; they list the references used in the preparation of the report including those sited in the reference section.

The tanker Esso Osaka is the most studied ship in the field of maneuvering [9, 10, 11, 12, 32], and it is used to test the accuracy of the additional features implemented into the present model.

4.1 Engine Model

The tanker Esso Osaka's power plant is a steam turbine with service horsepower rated at 35,000 hp at 81 rpm. The engine rpm, calculated according to Eq. 2.5 and 2.6, is hardly influenced by the operating conditions of the ship. Figure 4.1 shows the engine rpm versus time curve (solid line) of the ship starting at zero speed with engine commanded to 36 rpm, the engine reaches its command rpm readily even with the extreme propeller loading due to the ship's slow speed. Figure 4.1 also shows the rpm vs time curve (broken line) for a slow-speed diesel engine with identical horsepower; the response of the diesel power plant to engine command is much slower than the steam turbine. Good engine command response is characteristic of steam turbine power plants, and it is also evident in Inoue's data [33] that the rpm decrease in turn is substantially lower for ships with steam power plant than those with diesel engine.

In his report, Hooft [34] suggested an alternative method to determine the engine shaft horsepower SHP in Eq. 2.6. The torque Q_E delivered by the power plant is calculated from the power required to maintain the equilibrium speed u_E corresponds to the command engine rpm n_c, instead of using the maximum service horsepower. The resulting rpm vs time curve (dotted line) calculated according to this method is also shown in Figure 4.1, the rpm increase is remarkably slower than the one calculated according to Eq. 2.6.

4.2 Shallow Water

4.2.1 Shallow Water Effects on Resistance and Propeller Thrust

The shallow water effects on the longitudinal resistance and propeller thrust are modelled by Eq. 2.17 and 2.18, the modellings are verified by the rpm vs speed curves at deep, medium and shallow waters represented by the solid, broken and dotted line in Figure 4.2, respectively; they show the same trend as those obtained from the sea trial of Osaka [32].

4.2.2 Shallow Water Effects on Maneuverability

The shallow water effects on the maneuverability of ships are modelled by modifying the hydrodynamic derivatives, and the rudder parameters a_H, x_H and γ according to the draft to depth ratio T/h. Since this is achieved by adjusting their deep water values with polynomial functions f(T/h), the accuracy of the "adjusting" polynomials are essential to the correct modelling of shallow water effects. The linear hydrodynamic derivatives are adjusted according to Sheng's formulae and the non-linear derivatives are adjusted according to the polynomial presented by the curve shown in Figure 2.1. However, there are controversial regarding the values of the polynomial shown in Figure 2.1 at different T/h ratios; Table 4.1 shows the variations of f(T/h) for the non-linear derivatives derived theoretically by Zhu [9] and experimentally by Fujina [10], Yumuro [11] and Kijima [12] for Osaka. The three rudder parameters are adjusted according to the results published by Hirano [5].

Figure 4.3 compares the turning path of Osaka with 7 kt approach speed and 35° starboard rudder in deep water (dotted line), shallow water with only the linear derivatives adjusted (broken line), and shallow water with both linear and non-linear derivatives adjusted (solid line); and Figure 4.4 compares the heading angle versus time results of the 20°/20° zig-zag maneuver of Osaka with 7 kt approach speed for the same test combination. Because of the controversy regarding the shallow water values of non-linear hydrodynamic derivatives, the simulated turning circle and zig-zag maneuver results of Osaka cannot be compared quantitatively with those measured from the sea trial. Nevertheless, the simulated results in shallow water with both linear and non-linear derivatives adjusted show correctly the shallow effects on maneuverability [3]:

1. Turning diameter increases in shallow water, Figure 4.3;

2. Speed reduction due to maneuvering is less in shallow water than in deep water, as indicates by the ship speed versus time during the turning circle maneuver in deep water (dotted line) and shallow water (solid line) in Figure 4.5; and

3. The overshoot angle during zig-zag maneuver decreases in shallow water due to increase in dynamic stability.

Figure 4.3 and 4.4 also show the non-linear derivatives have significant influences on the shallow water behaviours as indicated by the differences between the results with the linear derivatives adjusted (broken line) only and those with both linear and non-linear derivatives adjusted (solid line).

4.3 Bank and Channel

The bank and channel effects are verified by examining the simulated motion of Osaka in a channel. Figure 4.6 shows the simulated ship path in the channel and Figure 4.7 shows the velocity parameters v and r. Initially, the ship is off-center, closer to the high-side (the side with higher y-coordinate), of the channel. Consequently, the bank suction force exerted attracts the ship toward the high-side and thecorresponding moment turns the bow counterclockwise thus decreasing the heading angle. These effects are shown in Figure 4.6 and 4.7, they indicate the ship moves to the high-side of the channel while the bow is turning toward the centerline, and with no rudder correction the ship will collide with the channel eventually.

4.4 Bow Thruster

The modelling of the bow thruster is tested for its ability to turn the ship and the ship speed effects on its effectiveness. The verification is based on the simulated results, Osaka is assumed to have a thruster with shaft horsepower of 1,750 hp, 5% of the main engine's. The ability of the bow thruster as a maneuvering aid is demonstrated in Figure 4.8 where the space requirements with and without thruster for Osaka to change heading 90° with 1 kt approach speed and 5° starboard rudder are shown. In Figure 4.8, Osaka with bow thruster assistance (solid line) reaches 90° heading with 453 m of advance (measured from the abscissa) and 356 m of transfer (measured from the ordinate); whereas the unassisted ship (broken line) reaches the same heading with more than 1,916m of advance and 1,180m of transfer. In Figure 4.9, the ship's turning paths, using the bow thruster only with 0° rudder approach speeds of 1 kt (solid line) and 4 kt (broken line), are compared. The corresponding advance, transfer and final heading angle are 425 m, 207 m and 59°, and 2034 m, 263 m and 22° after 1,000 s, for the 1 kt and 4 kt path, respectively. Thus the ship speed effects on the bow thruster effectiveness are clearly demonstrated.

4.5 Wind

The wind effects are verified using the estimated aerodynamic shape of Osaka. Figure 4.10 shows the ship path with an uniform wind of 10 m/s at 90° measured clockwise from the

x-axis. Because the superstructure is near the stern, the wind exerts a negative moment on the ship thereby turning it into the wind, as illustrated in the figure.

The wind effects are also demonstrated in Figure 4.11 from the turning paths (solid lines) with an uniform wind of 20 m/s at 90° with 7 kt approach speed and 35° starboard and port rudder, respectively. The turning paths (dotted lines) correspond to no wind with the same approach speed and rudder angle are also shown in the figure. For the starboard turn, the turning diameter with wind is bigger than the one with no wind; and the situation is reverse for the port turn. The deviations in the turning path are attributed to the wind induced moment discussed previously. In the starboard turn, the wind moment opposes the rudder moment at the beginning stage of the turn, similar to the situation in Figure 4.10. When the relative angle between the ship and wind exceeds 90°, the wind moment concurs the rudder moment until the relative angle is above 270°. This phenomenon is also revealed in the yaw rate of the turn, since the yaw rate can be related to the net moment exerted on the ship.[1] Figure 4.12 compares the yaw rate versus time for the starboard turn in Figure 4.11, the yaw rate with wind (solid line) is lower initially and it exceeds the yaw rate without wind (dotted line) as the turn progresses - due to the higher net moment experienced.

Similar explanation can be used to describe the surge velocity versus time curve and sway velocity versus time curve in Figure 4.13 and 4.14 for the starboard turn. The surge and sway velocities with wind are higher than those without wind because at the start of the turn the wind force components are in the positive surge and sway directions. The wind force causes higher accelerations and consequently velocities in the surge and sway direction.

4.6 Current

The current effects are incorporated into the equations of motion as described in Eq. 2.43 to 2.47. To verify the current effects, an inform current of 0.5 m/s at 90° measured clockwise from the x-axis is used. Figure 4.15 shows the linear drift path of Osaka with an approach speed of 7 kt and 0° rudder angle.

---

[1] Strictly speaking the yaw acceleration should be related with the net moment exerted on the ship not the yaw velocity which is the time integral of the yaw acceleration. But in this case the differences between the yaw acceleration with and without wind throughout the turn are small so that the yaw velocity can be used to relate net moment exerted.

Figure 4.16 compares the turning paths of the ship with 7 kt approach speed and 35° rudder with and without current, solid and dotted line, respectively. Similar to Figure 4.15, the ship drifts along the ordinate with the current velocity; therefore, the turning path in current is distorted into a smaller turning diameter.

5.0 CONCLUSIONS

Based on the findings of the previous section, the mathematical modellings and implementations of the effects of engine model, shallow water, bank and channel, bow thruster, wind and current in the maneuvering simulation model are correct. The simulated results of the different effects are in good agreement with those expected from actual ship operating under similar conditions. Therefore, the main objective of the project is achieved.

However, the modelling of the engine model will require minor tuning in order to decide on the most appropriate method to calculate the engine torque Q_E from the two methods documented.The procedure adapted in the maneuvering simulation model to model the shallow water effects is adequate since the results show the trends expected correctly. But in order to simulate these effects more accurately, the changes in the non-linear hydrodynamic derivatives with water depth must either be known explicitly or tuned according to maneuvering behaviours measured at different water depths. This is necessary since no empirical formula is available to estimate the non-linear hydrodynamic derivatives in shallow water and their influences on the shallow water maneuverability are significant, as shown in this report.

A reference source of maneuvering information is compiled in the bibliography section. However, a detail documentation of the model-scale and full-scale maneuvering test results and their corresponding ship particulars contained in these references is not feasible due to the time and budget constraint of the project.

The software is modified to allow tuning of the deep water hydrodynamic derivatives. The software modifications, including the tuning of the deep water hydrodynamic derivatives, achieved are documented in Part II of the report. The procedures to use the modified maneuvering simulation model programs are described in Part III of the report.

6.0 RECOMMENDATIONS

The following topics are recommended for future study:

1. To continue testing of the present maneuvering simulation model and expand its capability by including the modelling of slow speed, large drift angle and astern motion; features included in most other maneuvering simulation models.

2. To continue software development of the current maneuvering simulation model including: implementation of run-time graphics with display of the ship's path during simulation and other pertinent information; improvement of user-friendliness at the data entry and simulation command levels; and refinement of the program output file structure so that analysis of results can be implemented in an organized and effective fashion.

3. To conduct a separate study solely for the purpose of collecting and documenting of maneuvering data and the corresponding ship information, since it is not practical to link data collection with other study where the time and budget allocated for data collection are not specified.

4. To conduct experimental and theoretical studies whereby to refine the mathematical modelling of the maneuvering simulation model including: prediction of the non-linear hydrodynamic derivatives in shallow water, theoretical study of ship motion in a channel; and comparison study of the accuracy of different mathematical modellings of the hull-propeller-rudder interactions as recommended in the previous reports [1].

7.0 REFERENCES

1. NORDCO Limited, "Mathematical Simulation of Ship Maneuvering", NRC, IMD, Report # LM-HYD-47, October 1987; and "Mathematical Simulation of Ship Maneuvering, Part 2 - Program Verification and Study of Hull, Propeller and Rudder Interactions, March 1988.

2. van Lammeren, W.P.A., et. al., "The Wageningen B-Screw Series", SNAME Transactions, Vol. 77, 1976.

3. Hooft, J.P., "Maneuvering Large Ships in Shallow Water-I", Jounal of Navigation, Vol. 26, 1973.

4. Harvald, Sv. Aa., "Wake and Thrust Deduction at Extreme Propeller Loadings for a Ship Running in Shallow Water", TRINA, Vol. 119, 1977.

5. Hirano, M., et.al., "An Experimental Study on Maneuvering Hydrodynamic Forces in Shalllow Water", Transactions of West-Japan Society of Naval Archectict, No. 69, 1985.

6. Sheng, Z.Y., "Contribution to the Discussion of the Manoeuvrability Committee Report", Proceedings of the 16th ITTC, Vol. 2, 1981.

7. Fujino, M., "Experimental Studies on Ship Manoeuvrability in Restricted Waters", International Shipbuilding Progress", Vol. 15, No. 168, 1968.

8. Clark, D., et.al., "The Application of Manoeuvring Criteria in Hull Design Using Linear Theory", TRINA, Vol. 125, 1982.

9. Zhu, W.M., "On Semi-Empirical Prediction for Non-Linear Hydrodynamic Forces on Ship Hull in Shallow Water", Proceedings of 18th ITTC, Vol. 2, 1987.

10. Fujino, M. and Ishiguro, T., "A Study of the Mathematical Model Describing Maneuvring Motions in Shallow Water-Shallow Water Effects on Rudder-Effectiveness Parameters" (In Japanese), Journal of the Society of Naval Architects of Japan, Vol. 156, 1984.

11. Yumuro, A., "Some Experiments on Shallow Water Effects on Maneuvering Hydrodynamic Forces Acting on a Ship Model"(In Japanese), IHI Engineering Review, Vol. 25, 1985.

12. Kijima, K. et. al., "A Study on the Ship Manoeuvring Characteristic in Shallow Water", Transactions of the West-Japan Society of Naval Architects, No. 69, 1985.

13. Schwanecke, H., "On the Propulsion Quality of Ships Operating at Restricted Water Depth", Ocean Engineering, Vol. 16, 1979.

14. Harvald, Sv. Aa., Resistance and Propulsion of Ships, Wiley-Interscience Publication, 1983.

15. Mikelis, N.E., "On the Mathematical Modelling for Simulation of Ship Handling Behaviour in Deep or Shallow Waters and in Cannals", Proceedings of International Conference on Simulators, 1983.

16. Kose, K., "Prospect of New Generation of Manoeuvering Mathematical Model", Proceedings of the 9th International Marine Simulator Forum, August 1983.

17. Yumuro, A., "Some Experiments on Shallow Water Effects on Maneuvering Hydrodynamic Forces Acting on a Ship Model", IHI Engineering Review, Vol. 25, 1985.

18. Hirano, M., A Computer Program System for Ship Maneuvering Motion Prediction, Techical Bulletin TB-85-01, MITSUI Engineering and Shipbuilding Co., 1985.

19. Norrbin, N., Some Design Concepts for a Simulator Model of Ship Maneuvering in Deep and Confined Waters, Thesis, Kungliga Tekniska Hogskolan, Elanders Boktryckeri, 1971.

20. Norrbin, N., Theory and Observations on the Use of a Mathematical Model for Ship Manoeuvring in Deep and Confined Waters, SSPA Publication No. 68, 1971.

21. Norrbin, N., "Bank Clearance and Optimal Section Shape for Ship Canals", Proceedings of 26th International Navigation Congress, Section I, 1985.

22. Eda, H., "Directional Stability and Control of Ships in Restricted Channels", SNAME Transactions, Vol. 79, 1971.

23. Schoenherr, K.E., "Data for Estimating Bank Suction Effects in Restricted Water and on Merchant Ship Hulls", Proceedings of the 1st Symposium on Ship Maneuverability, DTMB Report 1461, 1960.

24. Ridley, D.E., "Observations on the Effect of Vessel Speed on Bow Thruster Performance", Marine Technology, January 1971.

25. Beveridge, J.L., "Design and Performance of Bow Thrusters", Marine Technology, October 1972.

26. Norrby, R., " The Effectiveness of a Bow Thruster at Low and Medium Ship Speeds", International Shipbuilding Progress, Vol. 14, No. 156, August 1976.

27. Isherwood, R.M., "Wind Resistance of Merchant Ships", TRINA, Vol. 115, 1973.

28. Wilson, P.A. and Lewis, G.D.W., "Predicting Ship Manoeuvring Characteristics for Preliminary Design", Proceedings of the Internationnal Conference, CADMO 86, 1986.

29. Hirano, M., "A Computer Program System for Ship maneuvering Motion Prediction", Technical Bulletin TB85-01, Mitsui Engineering and Shipbuilding Co., 1985.

30. Mikelis, N.E., "A Procedure for the Prediction of Ship Manoeuvring Response for Initial Design", Computer Applications in the Automation of Shipyard Operation and Ship Design V", Elsevier Science Publishers, 1985.

31. Franke, R., "Smooth Interpolation of Scattered Data By Local Thin Plate Splines", Computations of Mathematics with Applications, Vol. 8, No. 4, 1982.

32. Crane, C.L., Jr., "Maneuvering Trials of a 278,000 -DWT Tanker in Shallow and Deep Waters", SNAME Transactions, Vol. 87, 1979.

33. Inoue, S., et. al., "A Practical Calculation Method of Ship Maneuvering Motion", International Shipbuilding Progress, Vol. 28, 1981.

34. Hooft, J.P., "Design Information on the Ship Manoeuvrability", Part I, Report No. 45931-1-NS, NSMD, December 1984.

8.0 BIBLIOGRAPHY

Channel

Bindel, S., "Experiments on Ship Maneuverability in Canals as Carried Out in the Paris Model Basin", Proceedings of the 1st Symposium on Ship Maneuverability, DTMB Report 1461, 1960.

Brard, R., "Maneuvering of Ships in Deep Water, in Shallow Water and in Canals", SNAME Transactions, Vol. 59, 1951.

Dand, I.W., "Hydrodynamic Aspects of Shallow Water Collisions",

Eda, H., "Directional Stability and Control of Ships in Restricted Channels", SNAME Transactions, Vol. 79, 1971.

Eda, H., "Maneuvering Performance of Ships in Critical Channels", SNAME Transactions, Vol. 90, 1982.

Eda, H., "A Study of Shiphandling Performance in Restricted Water: Development and Validation of Computer Simulation Model", SNAME Transactions, Vol. 94, 1986.

Edstrand, H., Shallow Water Phenomena and Scale Model Research - Some First Experience from the SSPA Maritime Dynamics Laboratory, Publications of the Swedish State Shipbuilding Experimental Tank, Nr. 81, Goteborg, 1978.

Fujino, M., "Experimental Studies on Ship Manoeuvrability in Restricted Waters - Part I", International Shipbuilding Progress, Vol. 15, No. 168, 1968.

Fujino, M., "Experimental Studies on Ship Manoeuvrability in Restricted Waters - Part II", International Shipbuilding Progress, Vol. 17, No. 186, 1970.

Hsiung, C.C., "Computering Interaction Forces and Moments on a Ship in Restricted Waterways", International Shipbuilding Progress, Vol. 35, No. 403, 1988.

Kijima, K., "Manoeuvrability of Ship in Confined Water", Proceedings of the International Conference on Ship Manoeuvrability, Vol. 1, 1987.

Kijima, K., "Manoeuvrability of Ships in Narrow Waterway", Naval Architecture and Ocean Engineering, vol. 23, 1985.

Norrbin, N.H., "Bank Clearance and Optimal Section Shape for Ship Canals", Proceedings of the 26th International Navigation Congress, Section I, 1985.

Schofield, R.B., "Movement of Ships in Restricted Navigation Channels", Proceedings of Institution of Civil Engineers, Part 2, 1988.

Schoenherr, K.E., "Data for Estimating Bank Suction Effects in Restricted Water and on Merchant Ship Hulls", Proceedings of the 1st Symposium on Ship Maneuverability, DTMB, Report 1461, 1960.

Hydrodynamic Coefficients

Abkowitz, M.A., "Measurement of Ship Hydrodynamic Coefficients in Maneuvering from Simple Trials during Regular Operations", Proceedings of the 19th ATTC, Vol. 2, 1980.

Baar, J.J.M., "Computation by Finite Element Method of Hydrodynamic Coefficients of Ships in Shallow Water", International Shipbuilding Progress, Vol. 31, No. 357, 1984.

Beukelman, W., "Calculation-Methods of Hydrodynamic Coefficients of Ships in Shallow Water", International Shipbuilding Progress, Vol. 31, No. 359, 1984.

Cary, C.M., An Analytical Alternative to the Planar Motion Mechanism for a Ship in Shallow Water, University of Michigan, College of Engineering Report No. 224, July 1980.

Fujino, M., "The Effects of the Restricted Waters on the Added Mass of a Rectangular Cylinder", Proceedings of the 11th Symposium on Naval Hydrodynamics, March 1976.

Hooft, J.P., "Further Considerations on Mathematical Menoeuvring Models", Proceedings of the International Conference on Ship Manoeuvrability, Vol. 1, 1987.

Inoue, S., "Hydrodynamic Derivatives on Ship Manoeuvring", International Shipbuilding Progress, vol. 28, No. 321, 1981.

Kasai, H., "A Semi-empirical Approach to the Prediction of Manoeuvring Derivatives (1st Report)", Transactions of West Japan Society of Naval Architect, No. 58, 1979.

Kasai, H., "A Semi-empirical Approach to the Prediction of Manoeuvring Derivatives (2nd Report)", Transactions of West Japan Society of Naval Architect, No. 65, 1983.

Mikelis, N.E., "Calculations of Acceleration Coefficients and Correction Factors Associated with Ships Manoeuvring in Restricted Waters: Comparisons between Theory and Experiments", TRINA, Vol. 123, 1981.

Mikelis, N.E., "Calculations of Hydrodynamic Coefficients for a Body Manoeuvring in Restricted Waters using a Three Dimensional Method", TRINA, Vol. 123, 1981.

Mikelis, N.E., "Data for the Evaluation of the Acceleration Coefficients for Tankers Manoeuvring in Shallow and Deep Waters", Shipbuilding, Vol. 29, No. 339, 1982.

Motora, S., "On the Measurement of Added Mass and Added Moment of Inertia of Ships in Steering Motion", Proceedings of the 1st Symposium on Ship Maneuverability, DTMB Reprot 1461, 1960.

Pettersen, B., "Calculation of Potential Flow About Three-Dimensional Bodies in Shallow Water with Particular Application to Ship Maneuvering", Journal of Ship Research, Vol. 26, No. 3, 1982.

Yasukawa, H., "A Theoretical Study of Hydrodynamic Derivatives on Ship Maneuvering in Restricted Water", Journal of the Society of Naval Architects of Japan, Vol. 163, 1988.

Wind, H.G., "Computation of Ship Manoeuvring Coefficients International Shipbuilding Progress, Vol. 31, No. 361, 1984.

Zhu, W.M., "On Semi-Empirical Prediction for Non-Linear Hydrodynamic Forces on Ship Hull in Shallow Water", Proceedings of 18th ITTC, Vol. 2, 1987.

Maneuvering Data

Clarke, D., "Manoeuvring Trials with the 50,000 - ton deadweight Tanker 'British Bombardier' - Part 1 Stopping Trials", BSRA Report NS. 141, Naval Architecture Report No. 52, 1966.

Clarke, D., "Manoeuvring Trials with the 50,000 - ton deadweight Tanker 'British Bombardier' - Part 2 Steering", BSRA Report NS. 142, Naval Architecture Report No. 53, 1966.

Clarke, D., "Maneuvering Trials with the 193,000 - tonne D.W. Tanker 'Esso Bernicia'", BSRA Report NS. 295, Naval Architecture Report No. 81, 1970.

Crane, C.L., "Maneuvering Trials of a 278,000 - DWT Tanker in Shallow and Deep Waters", SNAME Transactions, Vol. 87, 1979.

Datta, I., "M.V. Federal Hunter - Manoeuvring Experiments with Model 396: Part 2 - Standard Manoeuvring", NRC, IMD, Report TR-HYD-11, March 1987.

Wan, T.D., "Summary of Sea Trial Data on Full-Scale Manoeuvring Tests", China Ship Scientific Research Centre, February 1986.

Propulsion and Resistance

Harvald, Sv. Aa., "Wake and Thrust Deduction at Extreme Propeller Loadings for a Ship Running in Shallow Water", TRINA, Vol. 119, 1977.

Isherwood, R.M., "Wind Resistance of Merchant Ships", TRINA, Vol. 115, 1973.

Schwanecke, H., "On the Propulsion Quality of Ships Operating at Restricted Water Depth", Ocean Engineering, Vol. 16, 1979.

Song, H.G., "Mathematical Modelling of Ship Speed-Loss Due to Wind and Seas", Proceedings of Oceans 87, October 1987.

Townsin, R.L., "Approximate Formulae for Speed Loss Due to Added Resistance in Wind and Waves", TRINA, Vol. 124, 1982.

van Lammeren, "The Wageningen B-Screw Series", SNAME Transactions, Vol. 177, 1976.

Shallow Water

Brard, R., "Maneuvering of Ships in Deep Water, in Shallow Water and in Canals", SNAME Transactions, Vol. 59, 1951.

Dand, I.W., "Hydrodynamic Aspects of Shallow Water Collisions", TRINA, Vol. 118, 1976.

Edstrand, H., Shallow Water Phenomena and Scale Model Research - Some First Experience from the SSPA Maritime Dynamics Laboratory, Publications of the Swedish State Shipbuilding Experimental Tank, Nr. 81, Goteborg, 1978.

Fujino, M., "Experimental Studies on Ship Manoeuvrability in Restricted Waters - Part I", International Shipbuilding Progress, Vol. 15, No. 168, 1968.

Fujino, M., "Experimental Studies on Ship Manoeuvrability in Restricted Waters - Part II", Internatinal Shipbuilding Progress, Vol. 17, No. 186, 1970.

Fujino, M., "Rudder Force and Manoeuvring Motions in Shallow Water", Proceedings of the International Conference on Ship Manoeuverability, Vol. 1, 1987.

Fujino, M., "A Study of the Mathematical Model Describing Manoeuvring Motions in Shallow Water-Shallow Water Effects on Rudder-Effectiveness Parameters" (In Japanese), Journal of the Society of Naval Architects of Japan, Vol. 156, 1984.

Hirano, M., "An Experimental Study on Maneuvering Hydrodynamic Forces in Shallow Water", Transactions of the West-Japan Society of Naval Architects, No. 69, 1985.

Hooft, J.P., "Manoeuvring Large Ships in Shallow Water - I", Journal of Navigation, Vol. 26, 1973.

Hooft, J.P., "Manoeuvring Large Ships in Shallow Water - II", Journal of Navigation, Vol. 26, 1973.

Kijima, K., "A Study on the Ship Manoeuvring Characteristics in Shallow Water" (In Japanese), Transactions of the West-Japan Society of Naval Architects, No. 69, 1985.

Norrbin, N.H., Theory and Observations on the Use of a Mathematical Model for Ship Manoeuvring in Deep and Confined Waters, SSPA Publication No. 68, Goteborb, 1971.

Sheng, Z.Y., "Contribution to the Discussion of the Manoeuvrability Committee Report", Proceedings of the 16th ITTC, Vol. 2, 1981.

Yoshimura, Y., "Mathematical Model for the Manoeuvring Ship Motion in Shallow Water" (In Japanese), Journal of the Kansai Society of Naval Architects, Vol. 200, 1986.

Yumuro, A., "Some Experiments on Shallow Water Effects on Maneuvering Hydrodynamic Forces Acting on a Ship Model" (In Japanese), IHI Engineer Review, Vol. 25, 1985.

Zhu, W.M., "On Semi-Empirical Prediction for Non-Linear Hydrodynamic Forces on Ship Hull in Shallow Water", Proceedings of 18th ITTC, Vol. 2, 1987.

Thruster

Beveridge, J.L., "Design and Performance of Bow Thrusters", Marine Technology, October 1972.

English, J.W., "The Design and Performance of Lateral Thrust Units for Ships Hydrodynamic Considerations", TRINA, Vol. 105, 1963.

Norrby, R., "The Effectiveness of a Bow Thruster at Low and Medium Ship Speeds", International Shipbuilding Progress, Vol. 14, No. 156, 1967.

Ridley, D.E., "Observations on the Effect of Vessel Speed on Bow Thruster Performance", Marine Technology, January 1971.

Taniguchi, K., "Investigations into the Fundamental Characteristics and Operating Performances of Side Thruster", Mitsubishi Technical Bulletin No. 35, May 1966.

LIST OF TABLES

	Table
Shallow Water Effects on a_H and x_H	2.1
Shallow Water Effects on γ	2.2
Aerodynamic Coefficients - Fore and Aft Force	2.3
Aerodynamic Coefficients - Lateral Force	2.4
Aerodynamic Coefficients - Yaw Moment	2.5
Variation of Non-Linear Derivatives with Depth	4.1

LIST OF FIGURES

	Figure
f(T/h) vs T/h for Non-Linear Hydrodynamic Derivatives	2.1
u_I/u_∞ vs $u_\infty/\sqrt{gh}$	2.2
u_h/u_I vs $\sqrt{A_x}/h$	2.3
Bank Force and Moment	2.4
C_F vs Y_{CL}/B	2.5
α vs h/T	2.6
x_c vs h/T	2.7
Bank Force and Moment - Centerline	2.8
C vs Pitch/Diameter Ratio	2.9
K_F and K_M vs u_∞/u_j	2.10
Definition of Check Points On Ship	2.11
Engine RPM vs Time	4.1
Engine RPM vs Ship Speed	4.2
Turning Path - Deep, Medium and Shallow Water	4.3
Heading Angle vs Time - Deep, Medium and Shallow Water	4.4
Ship Speed vs Time - Deep and Shallow Water	4.5
Ship Path - Channel	4.6
Motion Parameters in Channel	4.7
Turning Path - Bow Thruster	4.8
Ship Path - Bow Thruster	4.9
Ship Path - Wind	4.10

LIST OF FIGURES

	Figure
Turning Path - Wind	4.11
Yaw Rate vs Time - Wind	4.12
Surge Velocity vs Time - Wind	4.13
Sway Velocity vs Time - Wind	4.14
Ship Path - Current	4.15
Turning Path - Current	4.16

TABLE 2.1

Shallow Water Effects on a_H and x_H

T/h	Δa_H	x'_H
0	0	0.50
0.2	0.02	0.46
0.4	0.05	0.41
0.6	0.17	0.32
0.8	0.44	0.18

TABLE 2.2

Shallow Water Effects on γ

h/T	γ/γ_∞
∞	1.0
1.5	1.81
1.2	1.28

TABLE 2.3 Aerodynamic Coefficients - Fore and Aft Force

YWIND	A_o	A_1	A_2	A_3	A_4	A_5	A_6
0°	2.152	-5.00	0.243	-0.164	0	0	0
10°	1.714	-3.33	0.145	-0.121	0	0	0
20°	1.818	-3.97	0.211	-0.143	0	0	0.033
30°	1.965	-4.81	0.243	-0.154	0	0	0.041
40°	2.333	-5.99	0.247	-0.190	0	0	0.042
50°	1.726	-6.54	0.189	-0.173	0.348	0	0.048
60°	0.913	-4.68	0	-0.104	0.482	0	0.052
70°	0.457	-2.88	0	-0.068	0.346	0	0.043
80°	0.341	-0.91	0	-0.031	0	0	0.032
90°	0.355	0	0	0	-0.247	0	0.018
100°	0.601	0	0	0	-0.372	0	-0.020
110°	0.651	1.29	0	0	-0.582	0	-0.031
120°	0.564	2.54	0	0	-0.748	0	-0.024
130°	-0.142	3.58	0	0.047	-0.700	0	-0.028
140°	-0.677	3.64	0	0.069	-0.529	0	-0.032
150°	-0.723	3.14	0	0.064	-0.475	0	-0.032
160°	-2.148	2.56	0	0.081	0	1.27	-0.027
170°	-2.707	3.97	-0.175	0.126	0	1.81	0
180°	-2.529	3.76	-0.174	0.128	0	1.55	0

TABLE 2.4 Aerodynamic Coefficients - Lateral Force

YWIND	B_o	B_1	B_2	B_3	B_4	B_5	B_6
0°	0	0	0	0	0	0	0
10°	0.096	0.22	0	0	0	0	0
20°	0.176	0.71	0	0	0	0	0
30°	0.225	1.38	0	0.023	0	-0.29	0
40°	0.329	1.82	0	0.043	0	-0.59	0
50°	1.164	1.26	0.121	0	-0.242	-0.95	0
60°	1.163	0.96	0.101	0	-0.177	-0.88	0
70°	0.916	0.53	0.069	0	0	-0.65	0
80°	0.844	0.55	0.082	0	0	-0.54	0
90°	0.889	0	0.138	0	0	-0.66	0
100°	0.799	0	0.155	0	0	-0.55	0
110°	0.797	0	0.151	0	0	-0.55	0
120°	0.996	0	0.184	0	-0.212	-0.66	0.34
130°	1.014	0	0.191	0	-0.280	-0.69	0.44
140°	0.784	0	0.166	0	-0.209	-0.53	0.38
150°	0.536	0	0.176	-0.029	-0.163	0	0.27
160°	0.251	0	0.106	-0.022	0	0	0
170°	0.125	0	0.046	-0.012	0	0	0
180°	0	0	0	0	0	0	0

TABLE 2.5 Aerodynamic Coefficients - Yaw Moment

YWIND	C_o	C_1	C_2	C_3	C_4	C_5
0°	0	0	0	0	0	0
10°	0.0596	0.061	0	0	0	-0.074
20°	0.1106	0.204	0	0	0	-0.170
30°	0.2258	0.245	0	0	0	-0.380
40°	0.2017	0.457	0	0.0067	0	-0.472
50°	0.1759	0.573	0	0.0118	0	-0.523
60°	0.1925	0.480	0	0.0115	0	-0.546
70°	0.2133	0.315	0	0.0081	0	-0.526
80°	0.1827	0.254	0	0.0053	0	-0.443
90°	0.2627	0	0	0	0	-0.508
100°	0.2102	0	-0.0195	0	0.0335	-0.492
110°	0.1567	0	-0.0258	0	0.0497	-0.457
120°	0.0801	0	-0.0311	0	0.0740	-0.396
130°	-0.0189	0	-0.0488	0.0101	0.1128	-0.420
140°	0.0256	0	-0.0422	0.0100	0.0889	-0.463
150°	0.0552	0	-0.0381	0.0109	0.0689	-0.476
160°	0.0881	0	-0.0306	0.0091	0.0366	-0.415
170°	0.0851	0	-0.0122	0.0025	0	-0.220
180°	0	0	0	0	0	0

TABLE 4.1 Variation of Non-Linear Derivatives with Depth

	Y'_{vv}		N'_{vrr}			N'_{vvr}		
T/h	Kijima	Zhu	Fujino	Kijima	Yumuro	Fujino	Kijimo	Yumuro
0.2	-	1.08	-	-	-	-	-	-
0.36	-	-	1.06	-	-	0.55	-	-
0.40	-	1.46	-	-	2.47	-	-	1.07
0.50	2.66	-	-	1.81	-	-	0.97	-
0.60	-	2.38	-	-	-	-	-	-
0.67	4.84	-	1.23	3.13	4.28	6.22	0.73	1.97
0.77	5.76	-	-	2.82	-	-	0.61	-
0.80	-	1.38	-	-	-	-	-	-
0.83	4.62	-	1.47	2.16	4.59	13.46	3.54	0.16

Figure 2.1

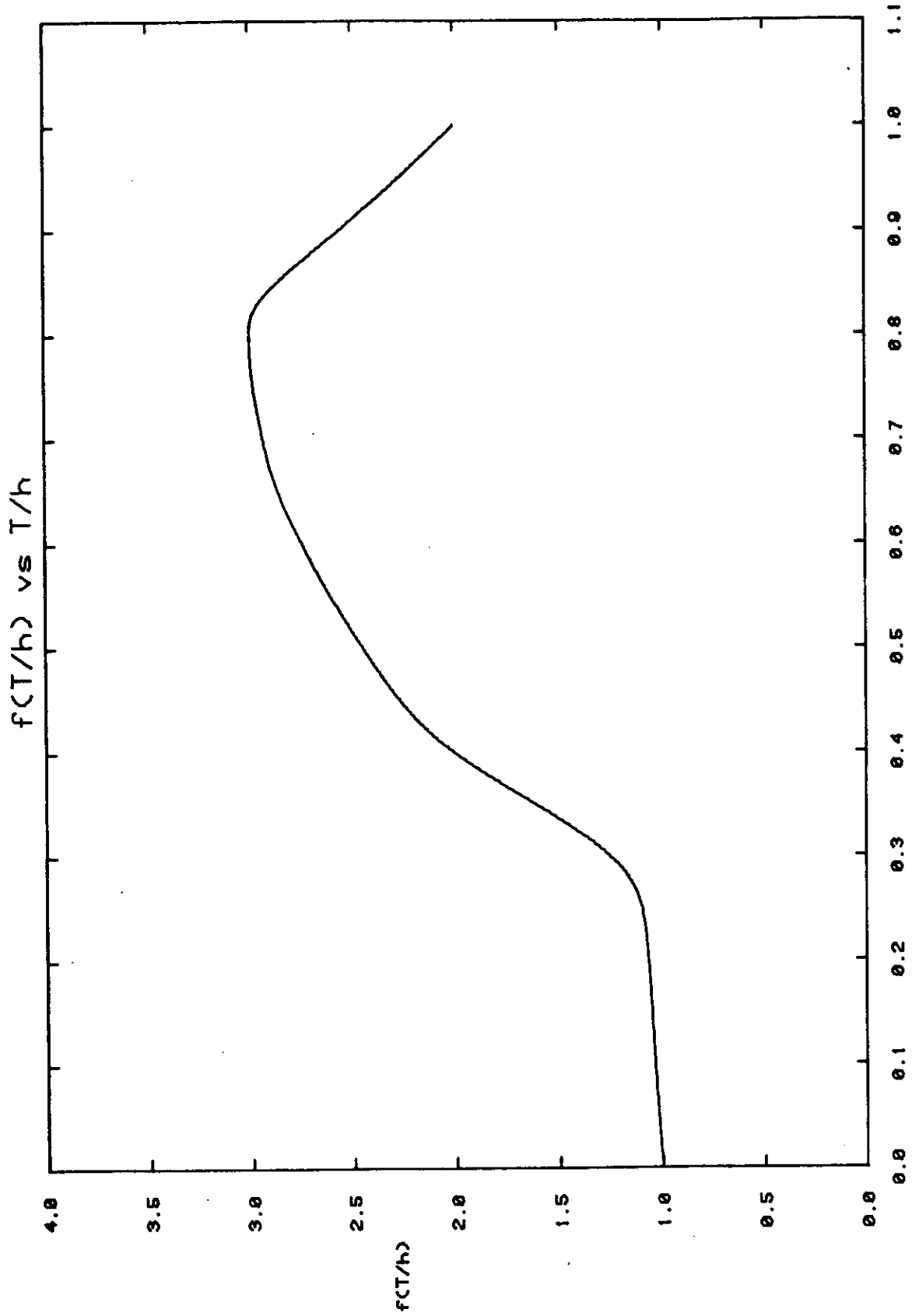

f(T/h) vs T/h for Non-linear Hydrodynamic

Figure 2.2

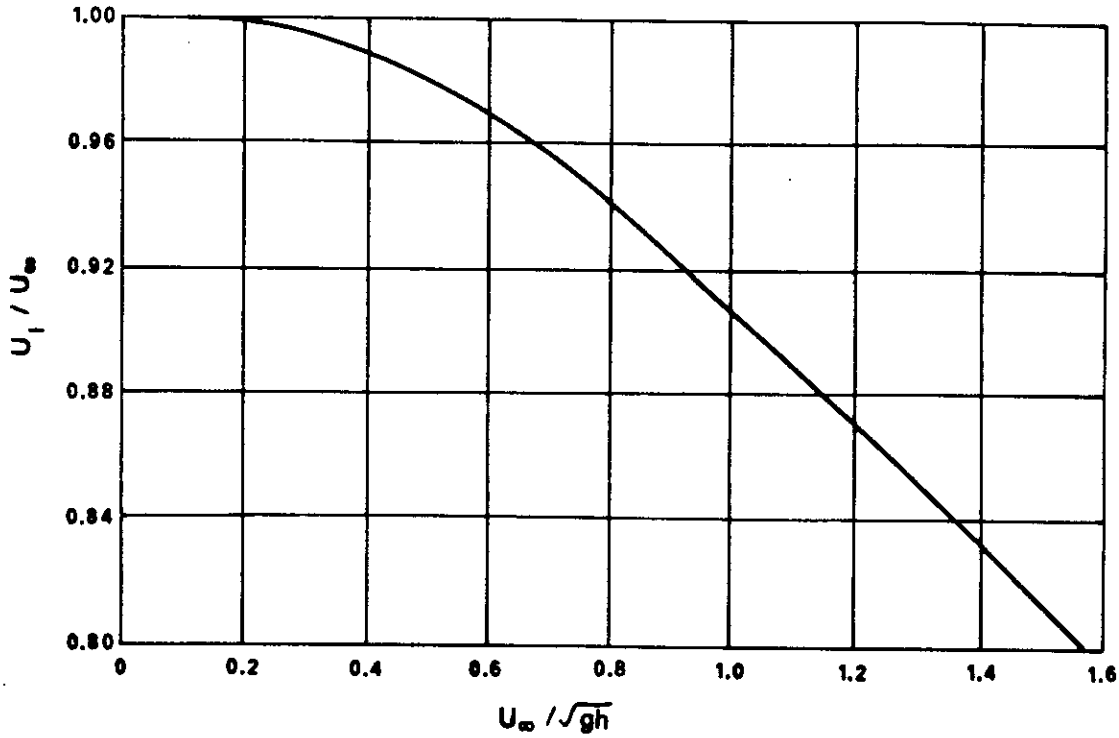

u_I / u_∞ vs $u_\infty / \sqrt{gh}$

Figure 2.3

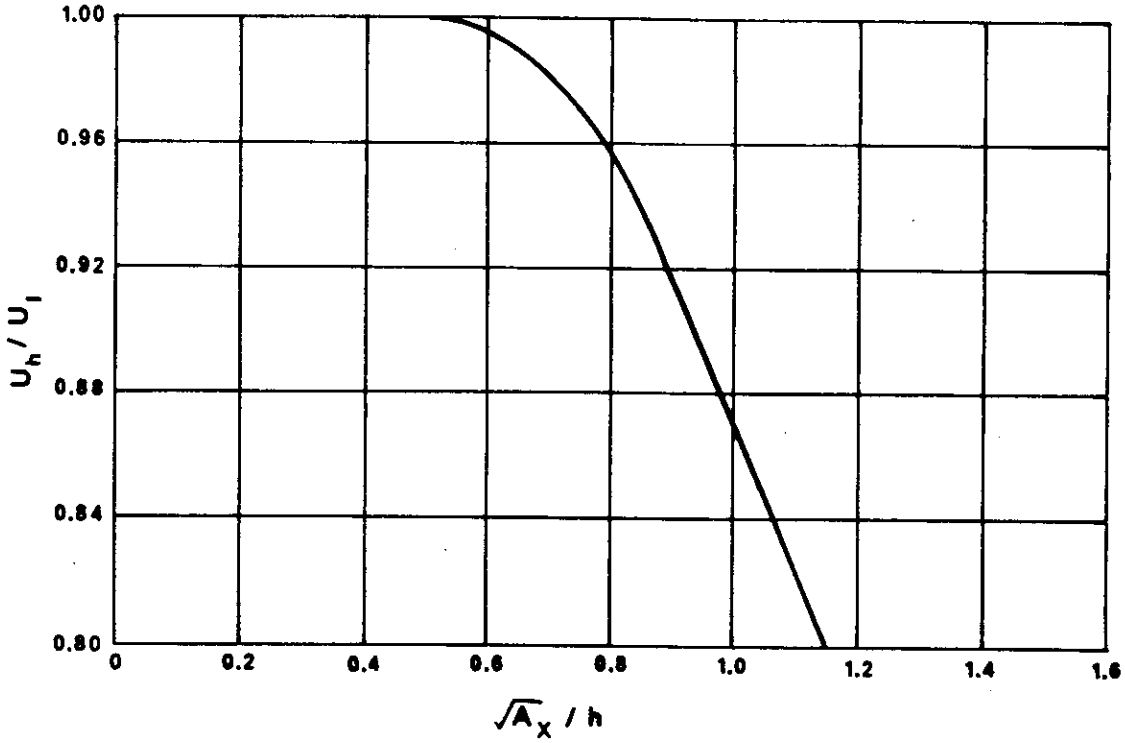

u_h / u_I vs $\sqrt{A_x} / h$

Figure 2.4

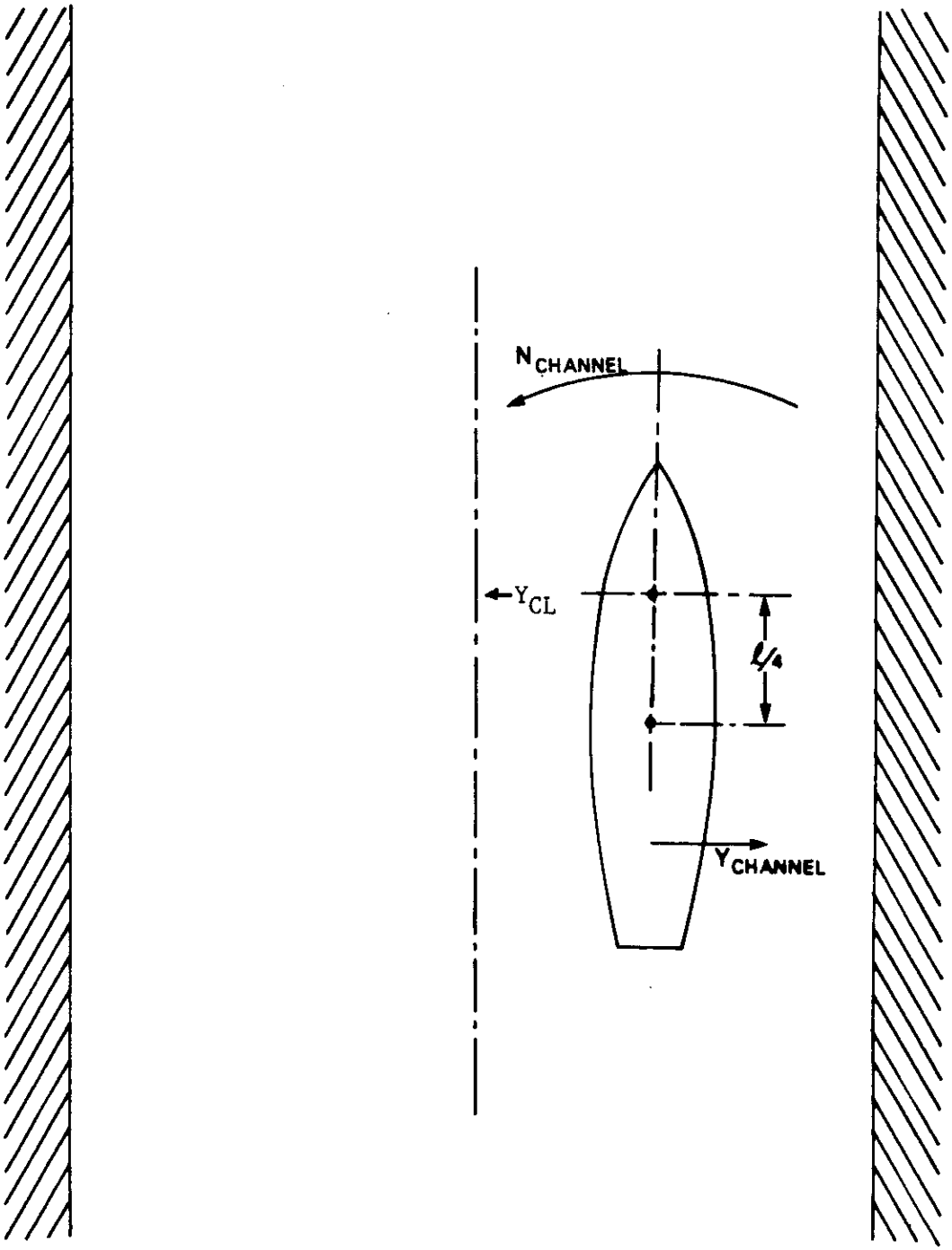

Bank Force and Moment

Figure 2.5

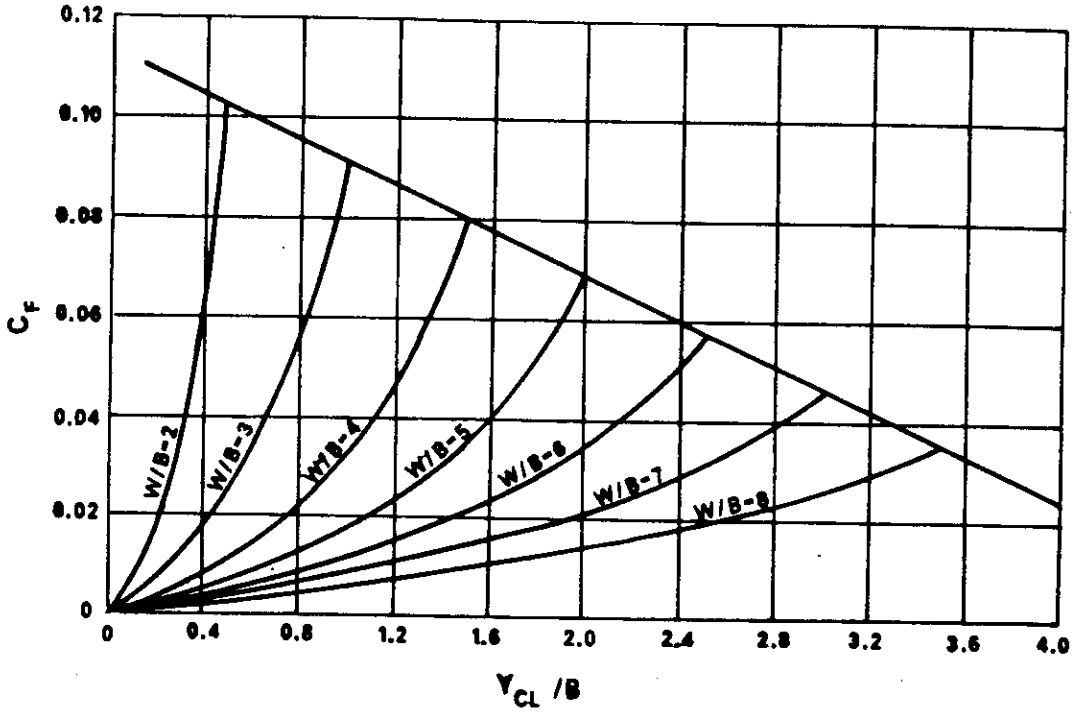

C_F vs Y_{CL} /B

Figure 2.6

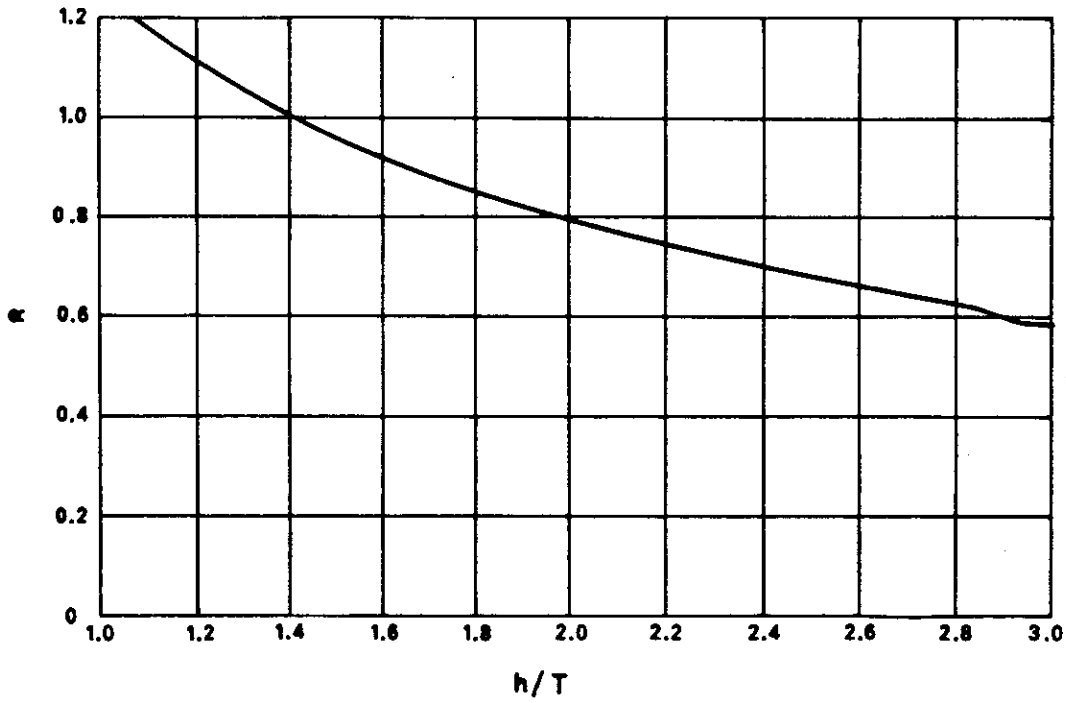

α vs h/T

Figure 2.7

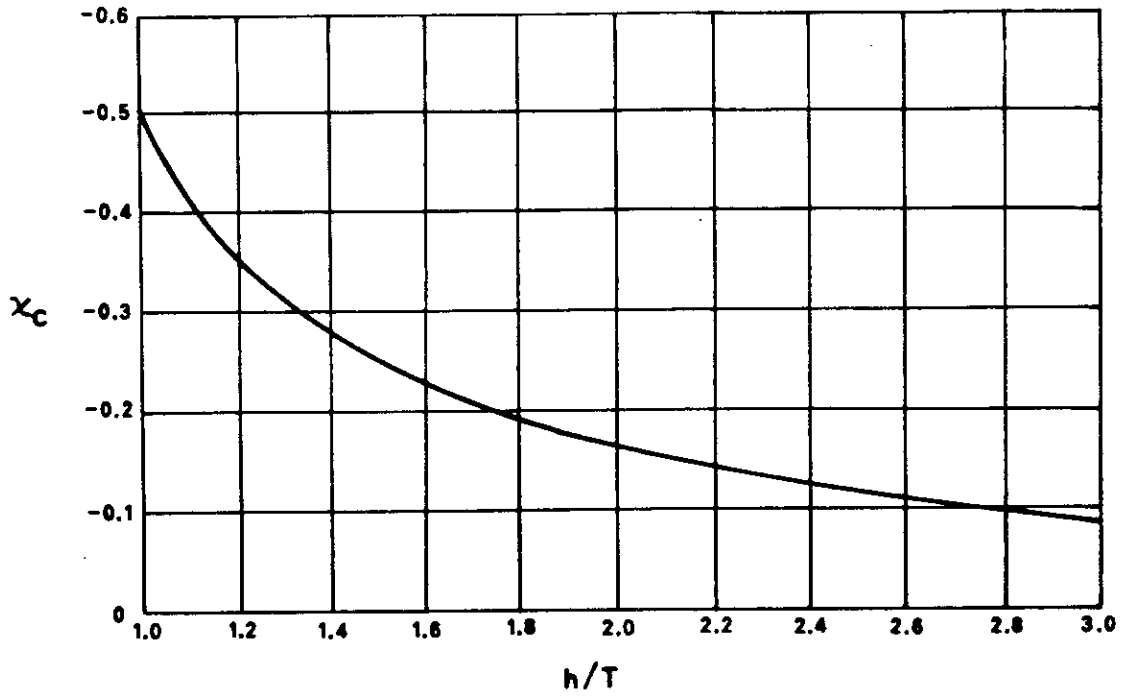

x_c vs h/T

Figure 2.8

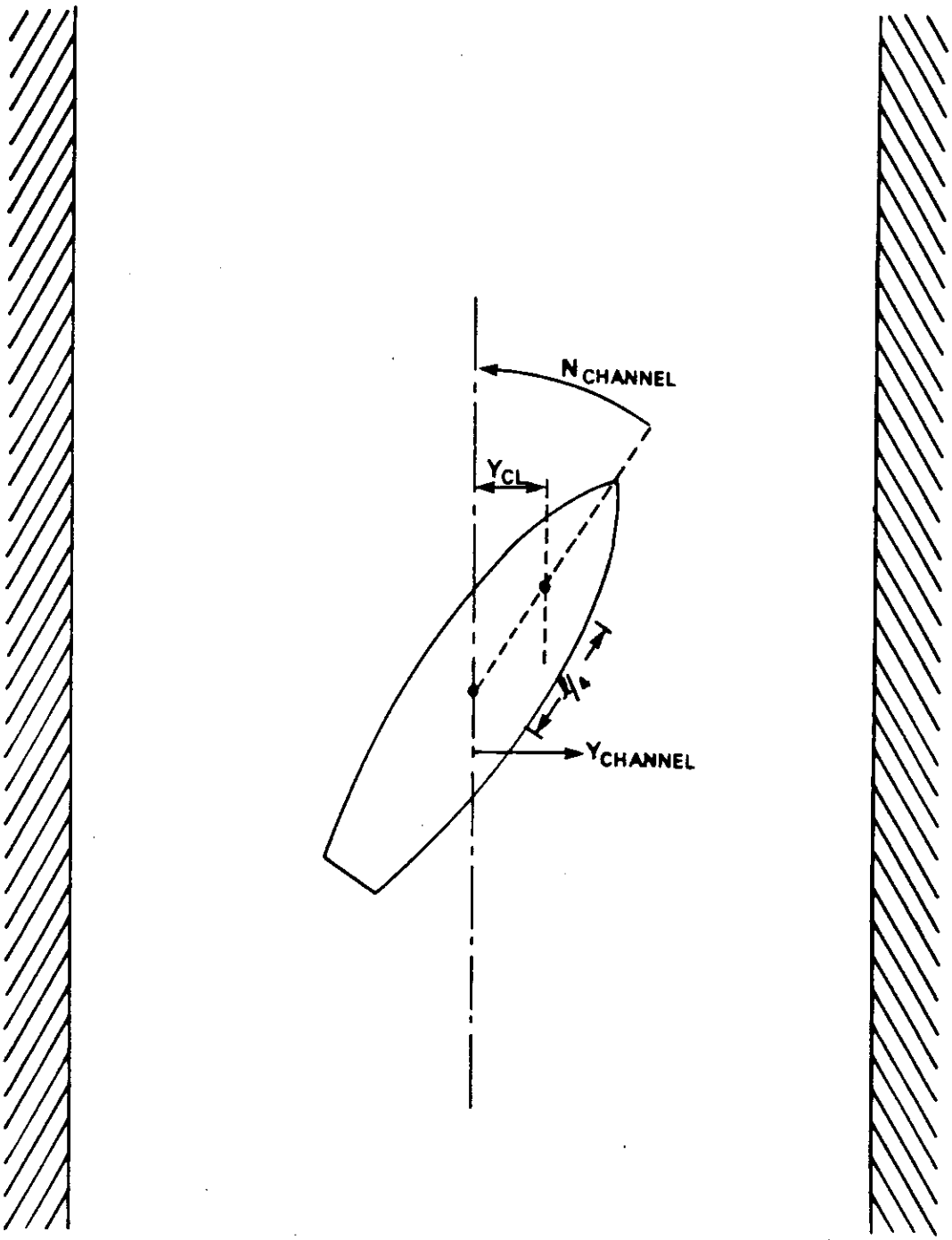

Bank Force and Moment - Centerline

Figure 2.9

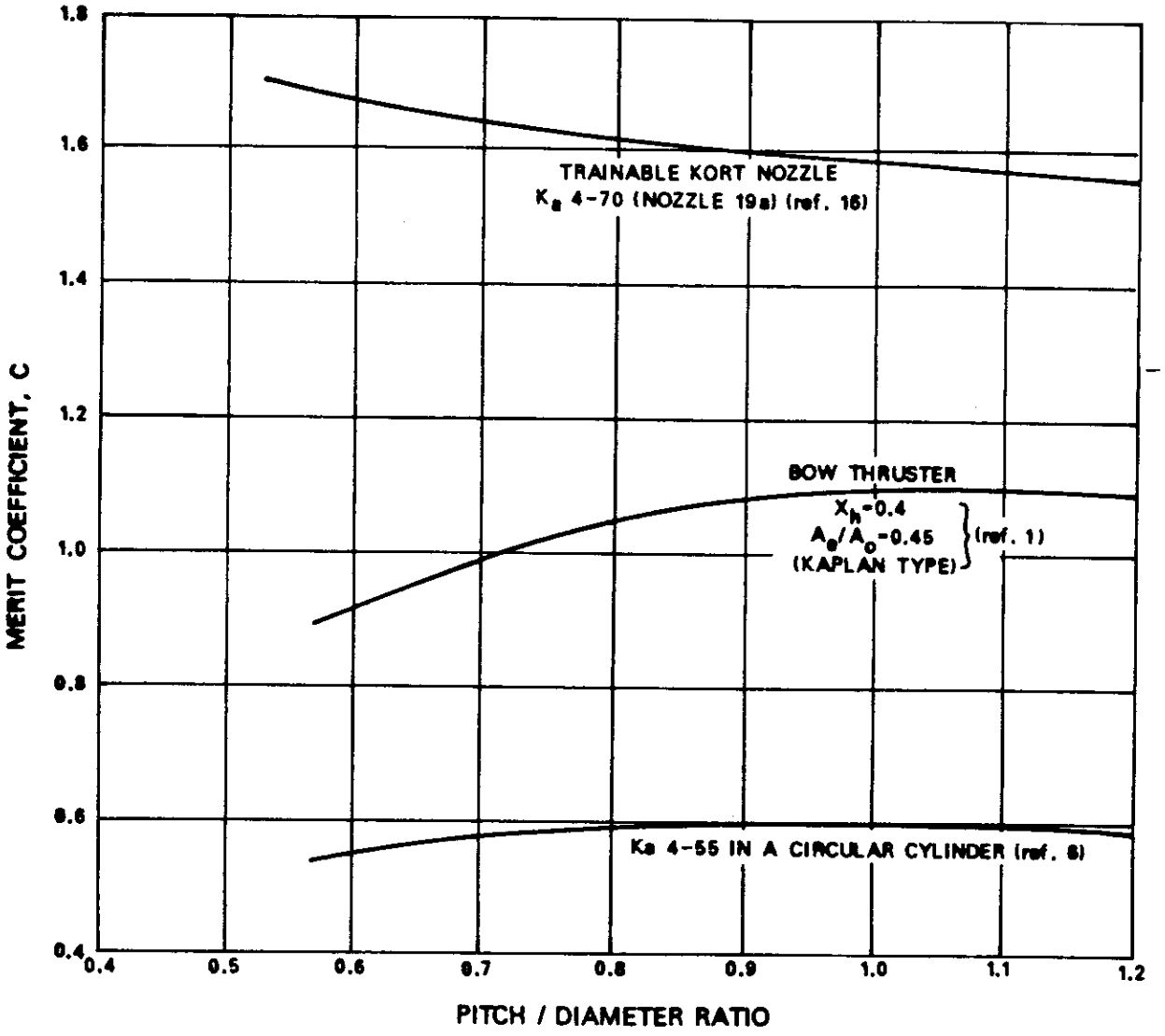

C vs Pitch/Diameter Ratio

Figure 2.10

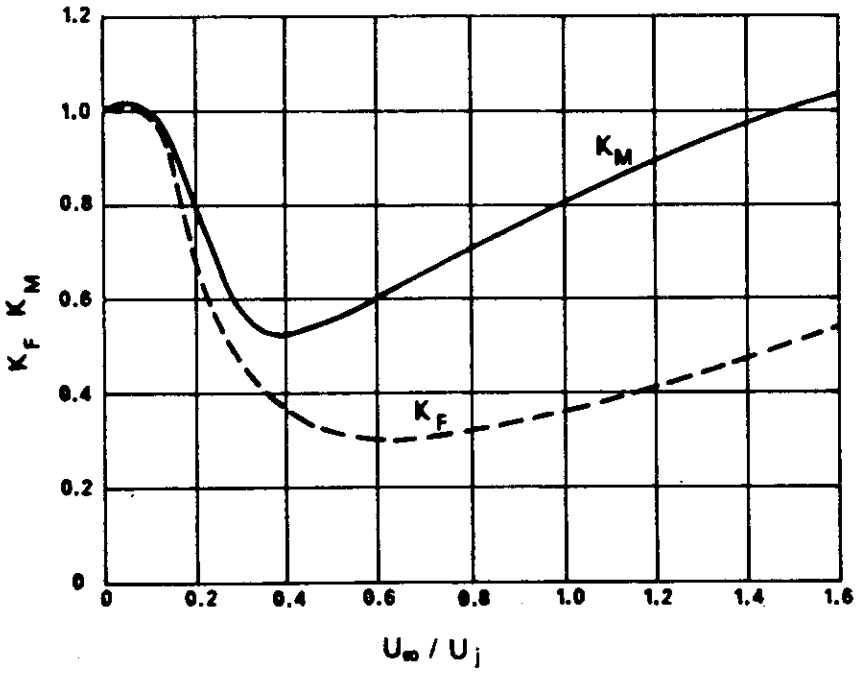

K_F and K_M vs u_∞/u_j

Figure 2.11

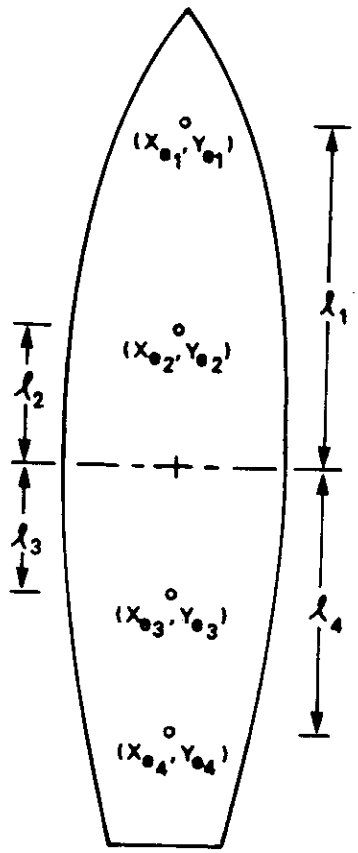

Definition of Check Points on Ship

Figure 4.1

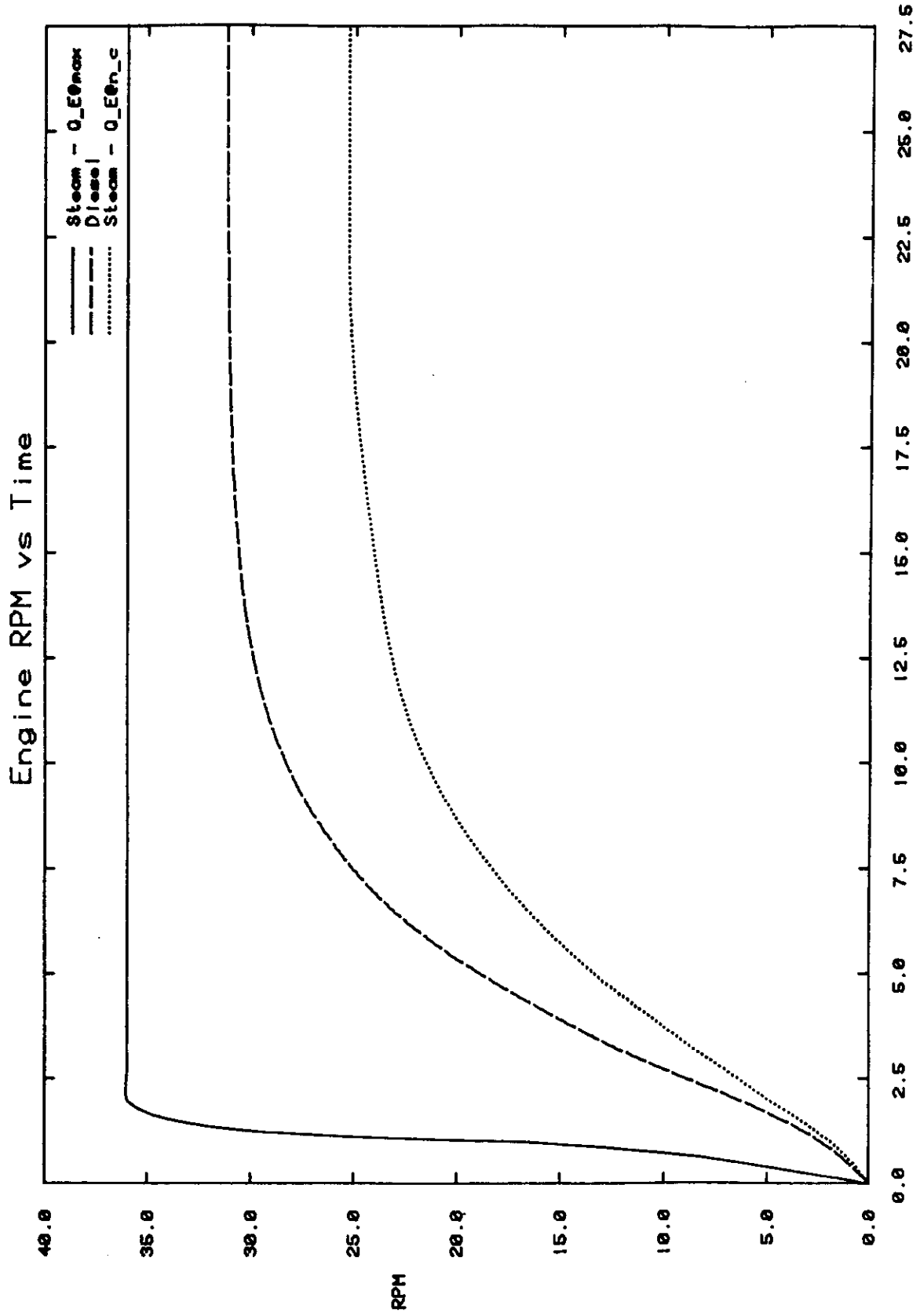

Engine RPM vs Time

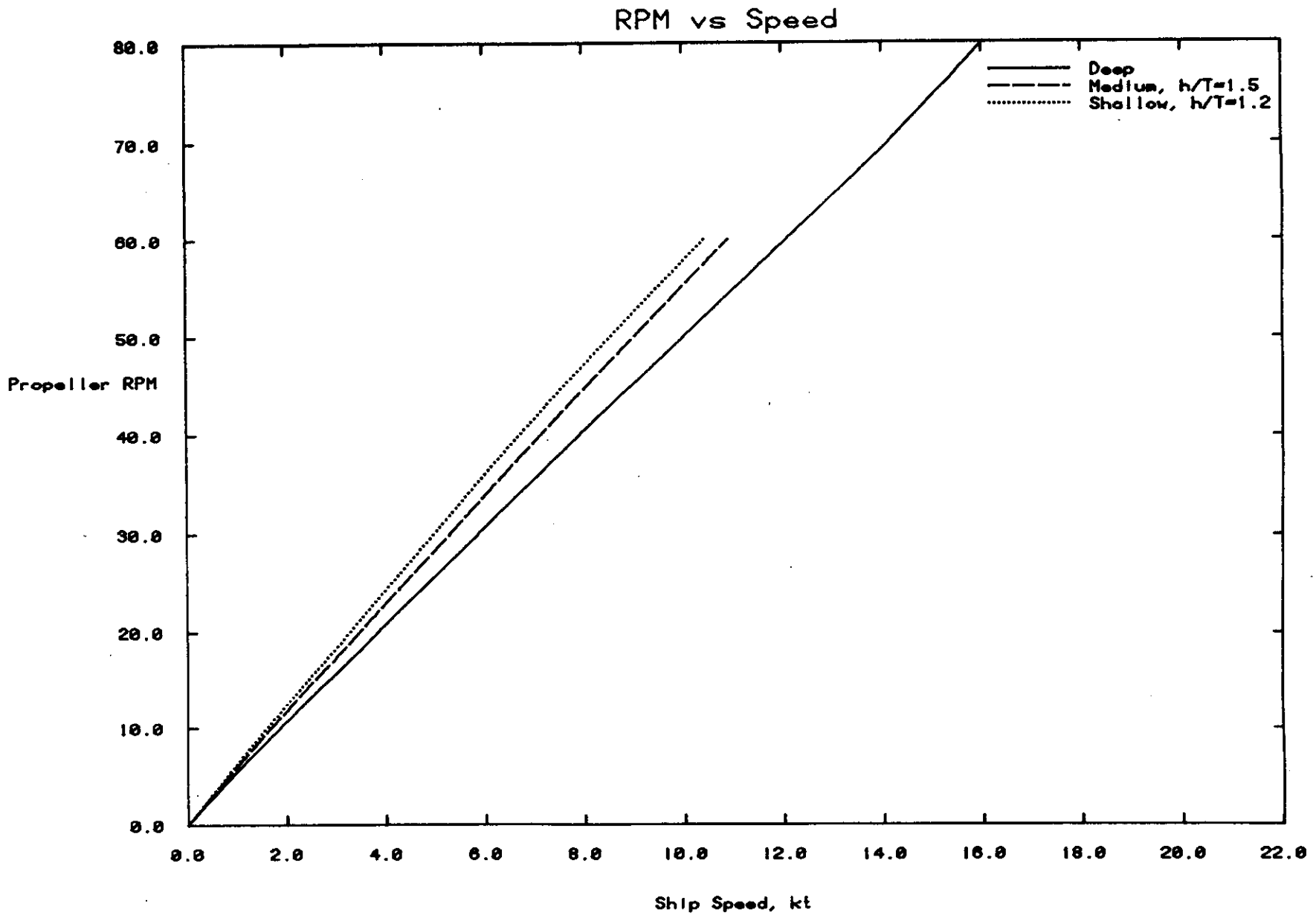

Engine RPM vs Ship Speed

Figure 4.2

Figure 4.3

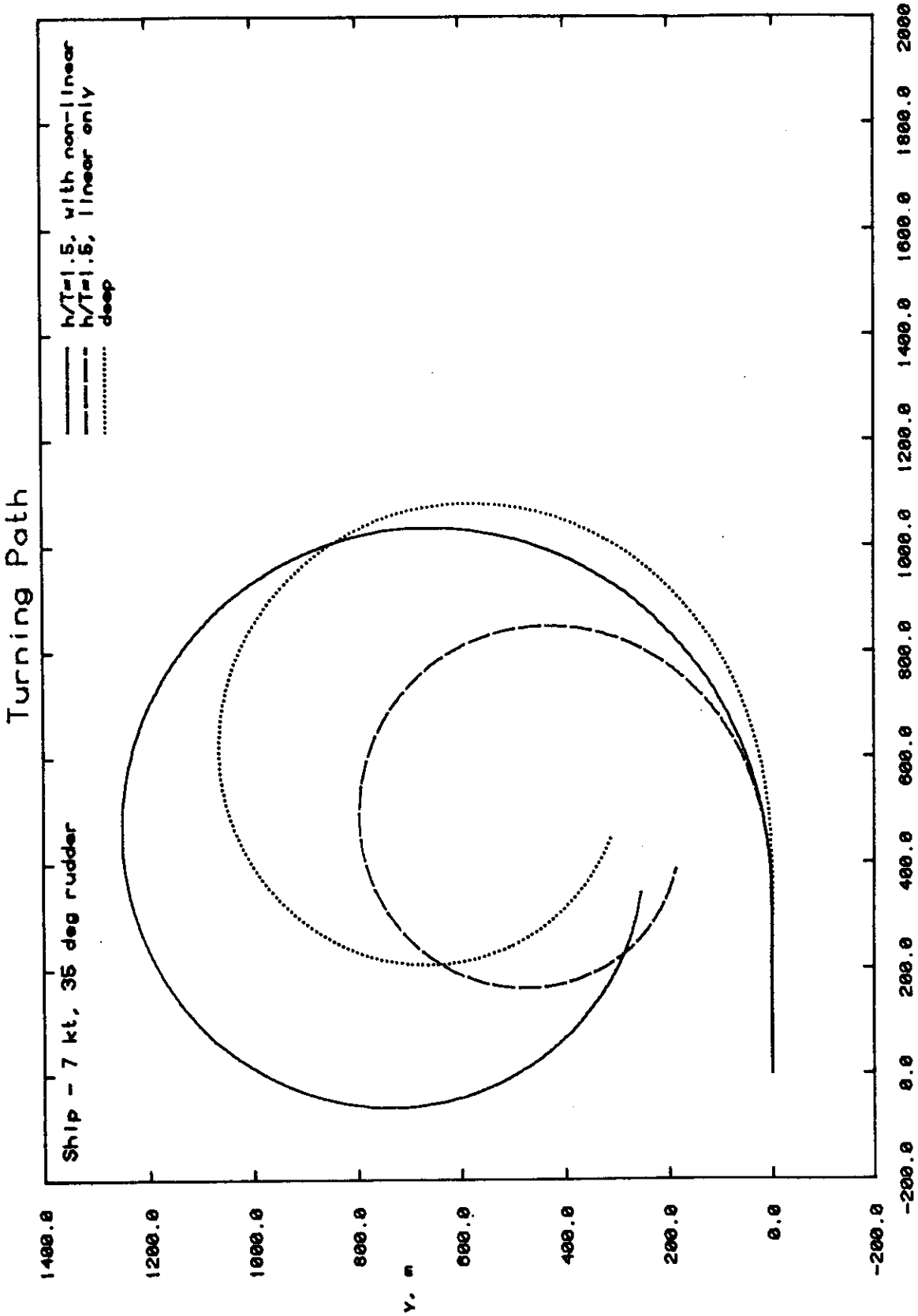

Turning Path - Deep, Medium and Shallow Water

Figure 4.5

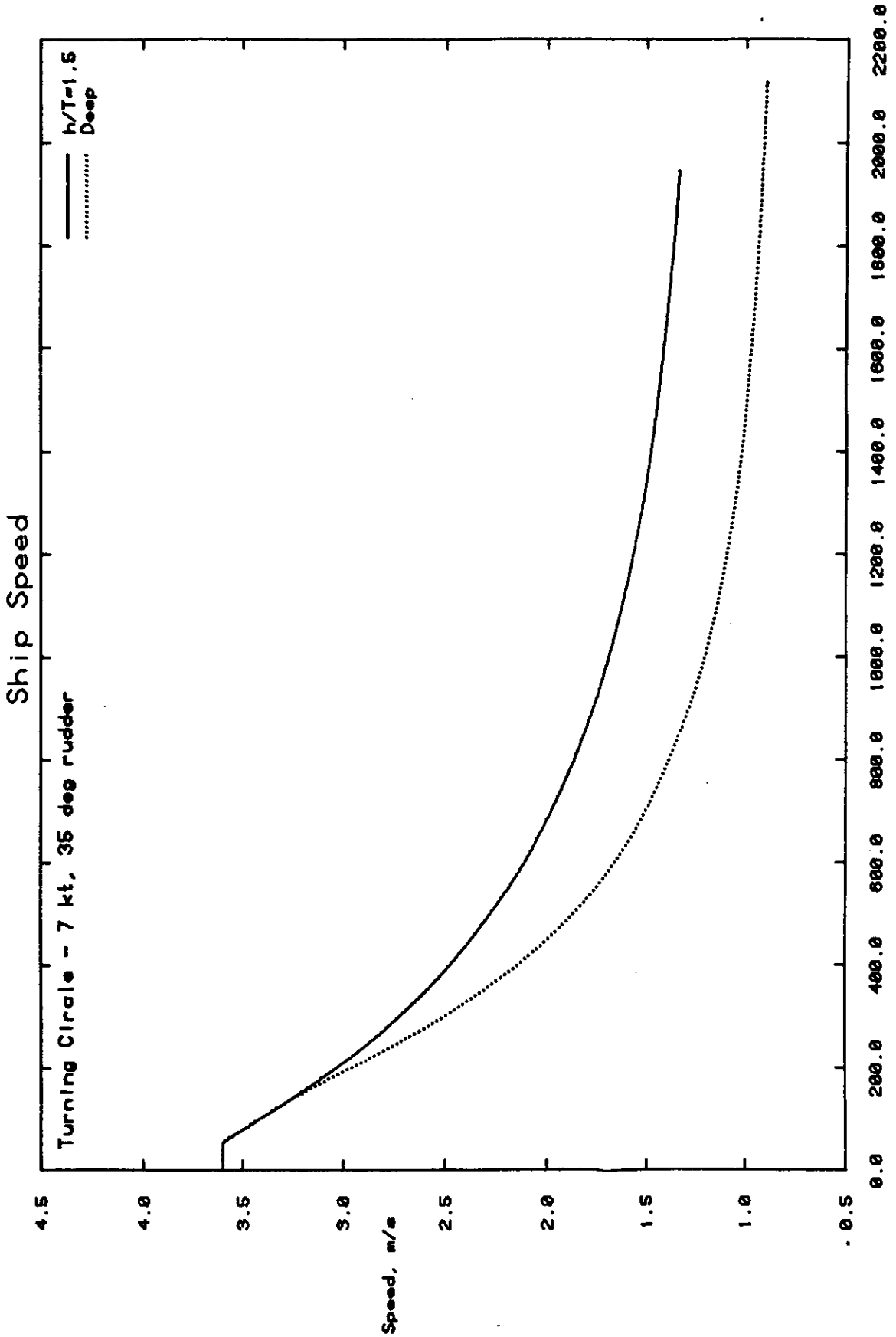

Ship Speed vs Time - Deep and Shallow Water

Figure 4.6

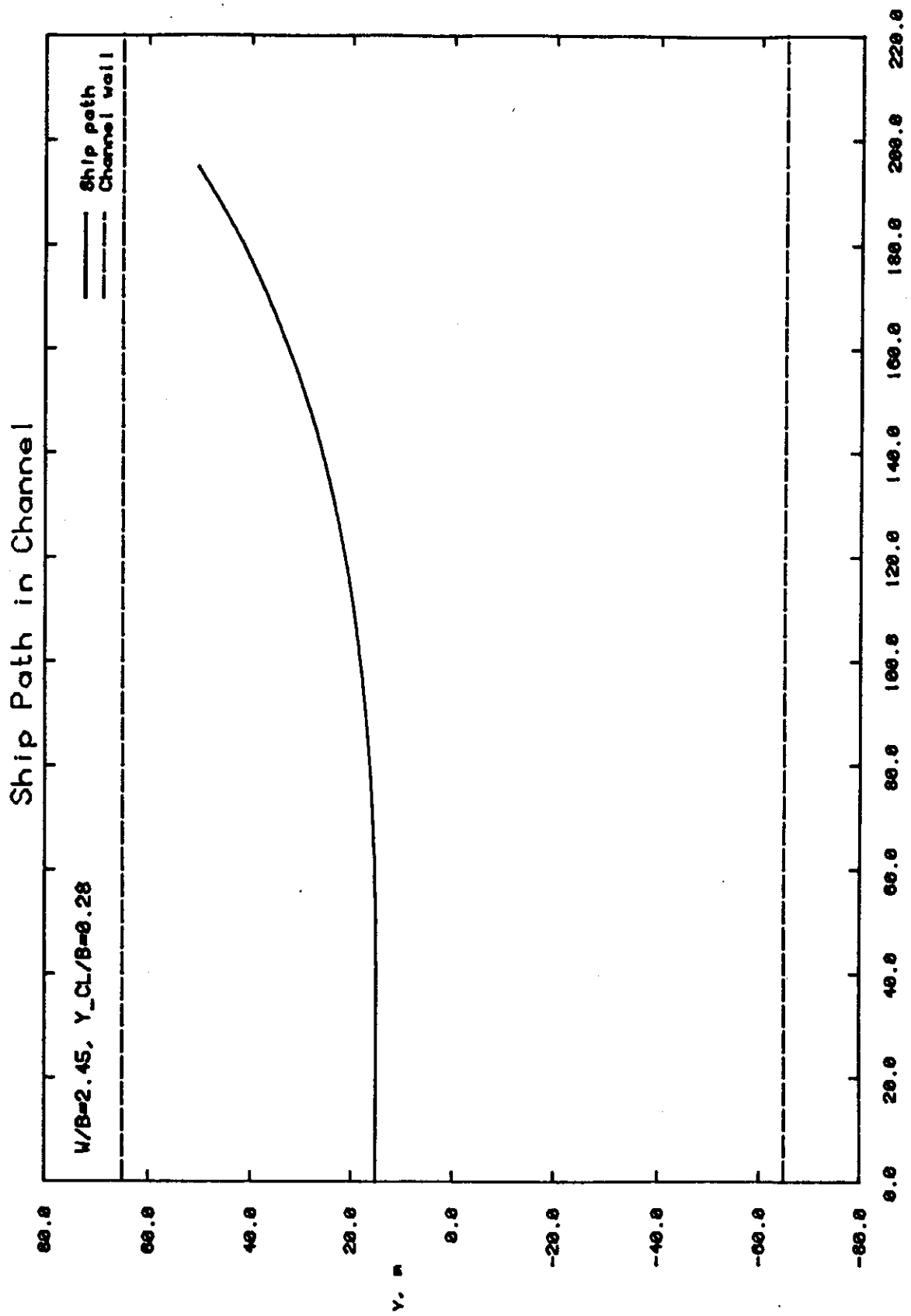

Ship Path - Channel

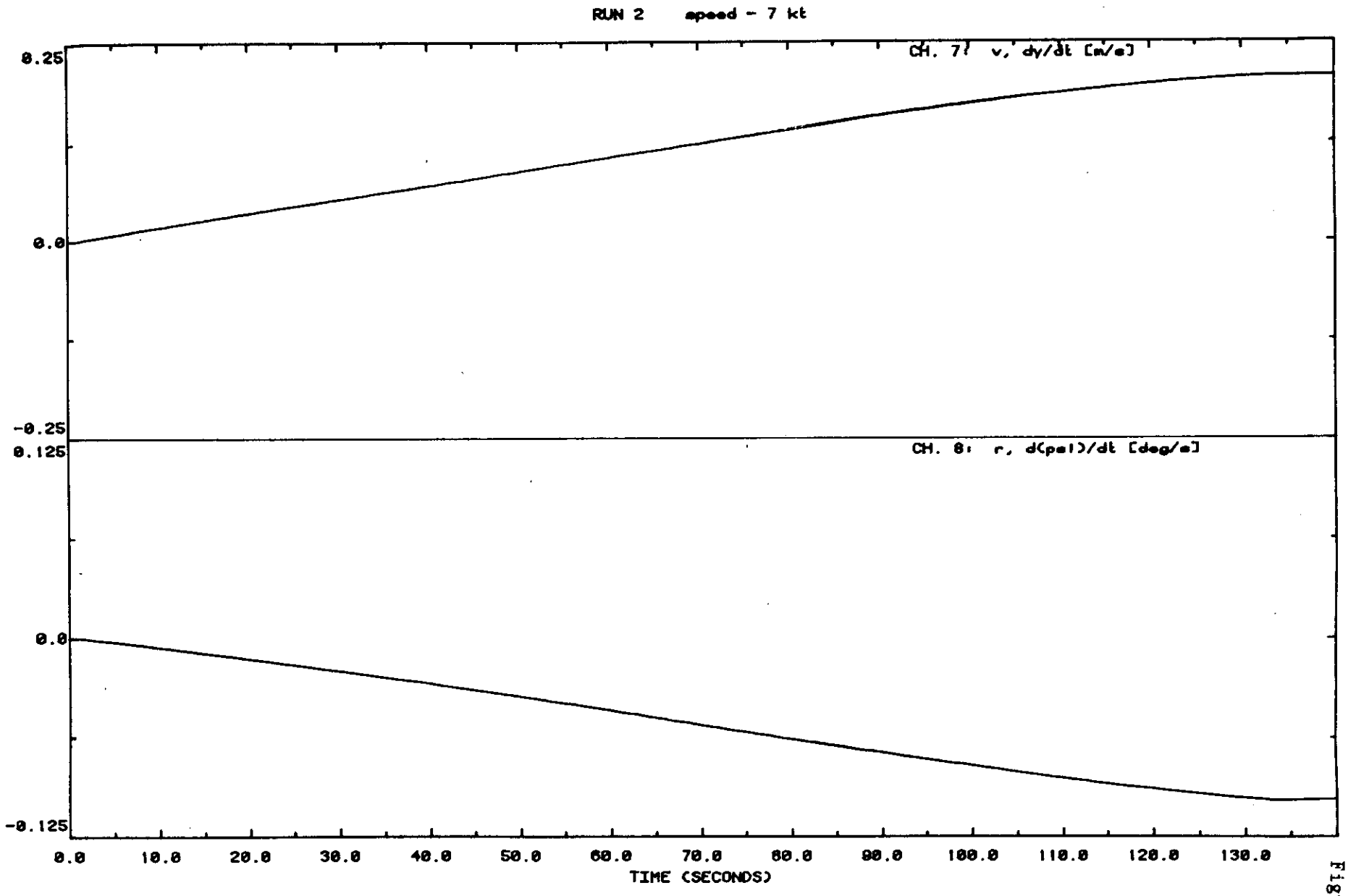

Figure 4.7

Motion Parameters in Channel

Figure 4.8

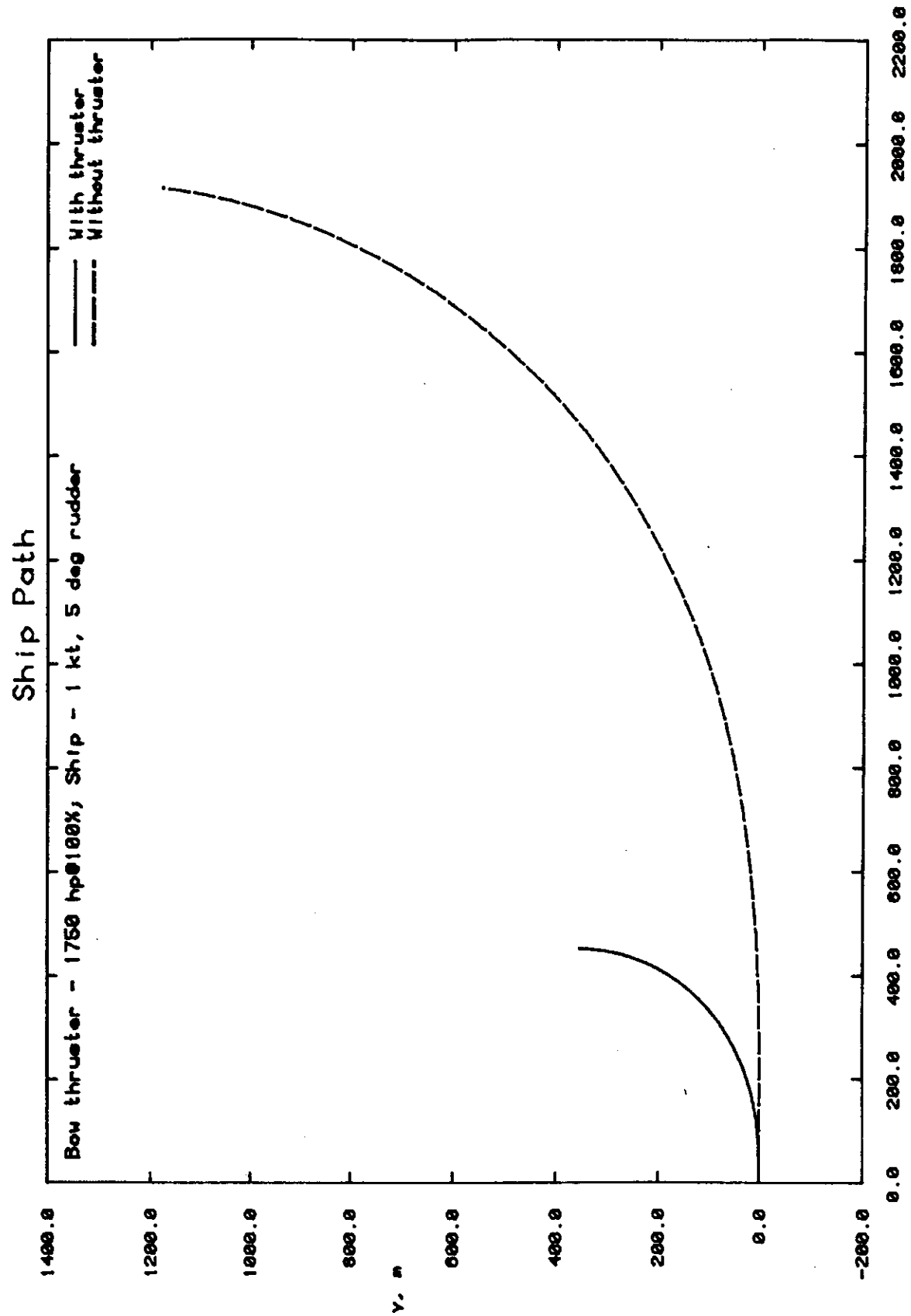

Turning Path - Bow Thruster

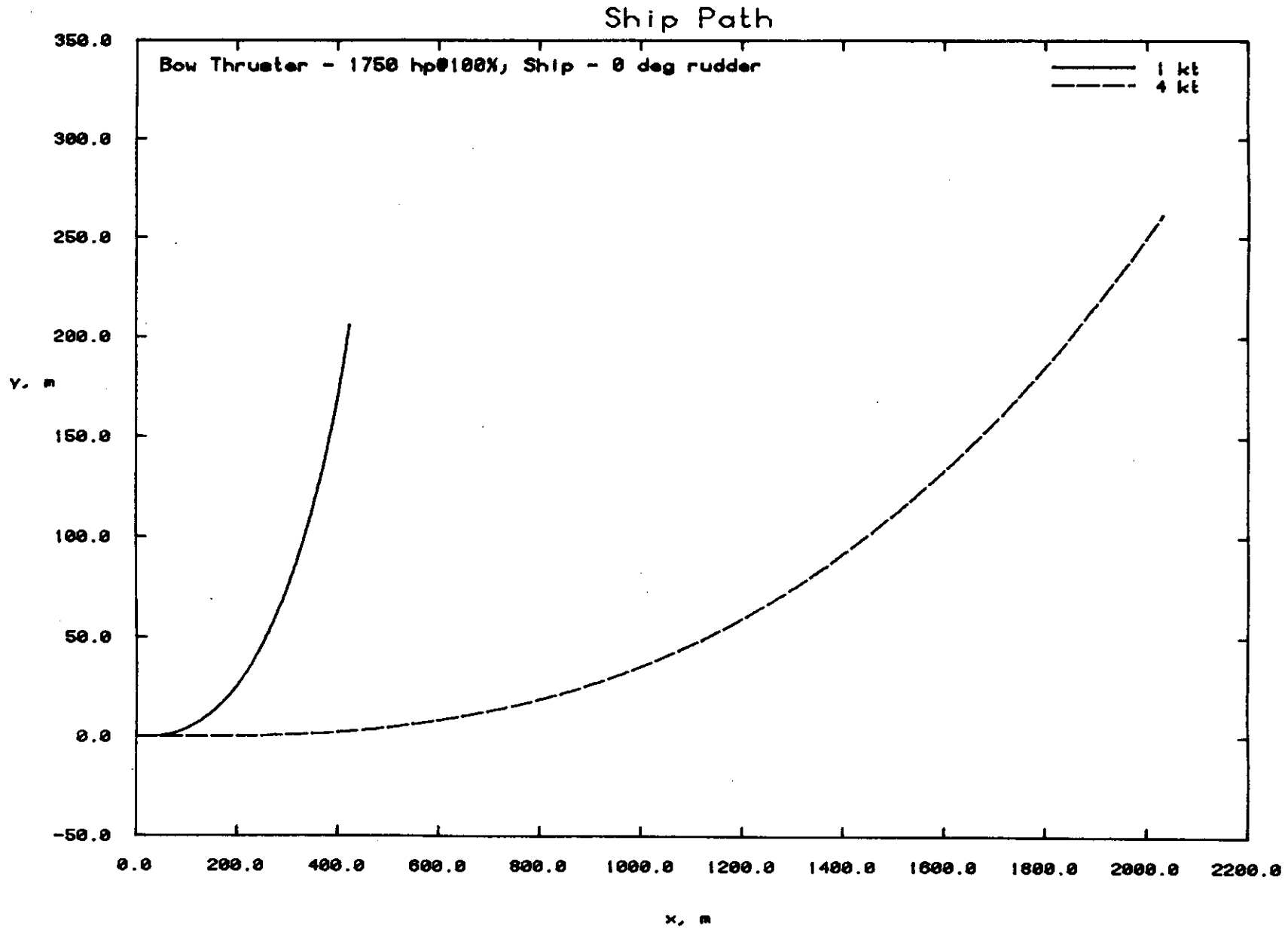

Ship Path - Bow Thruster

Figure 4.9

Figure 4.10

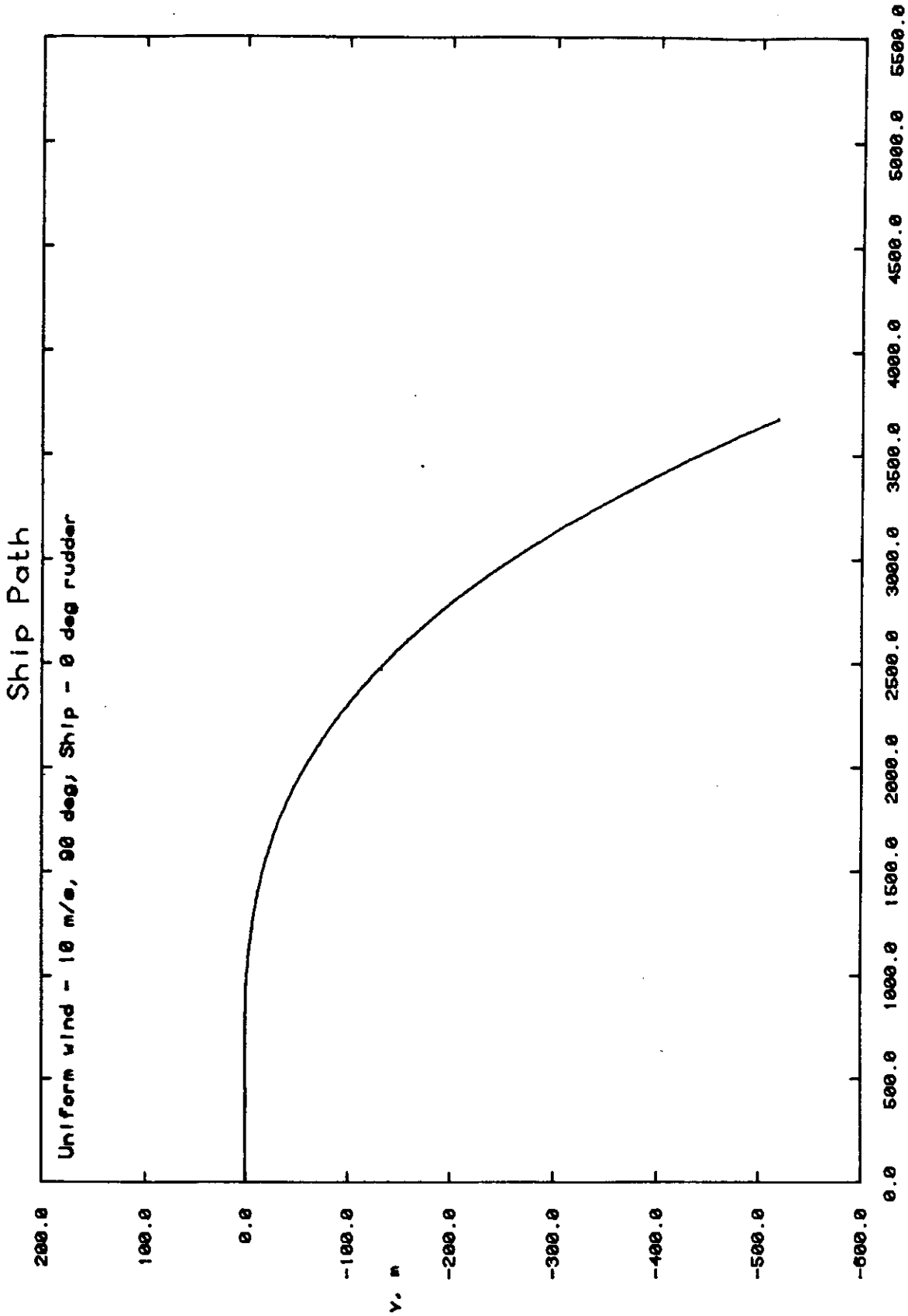

Ship Path - Wind

Figure 4.11

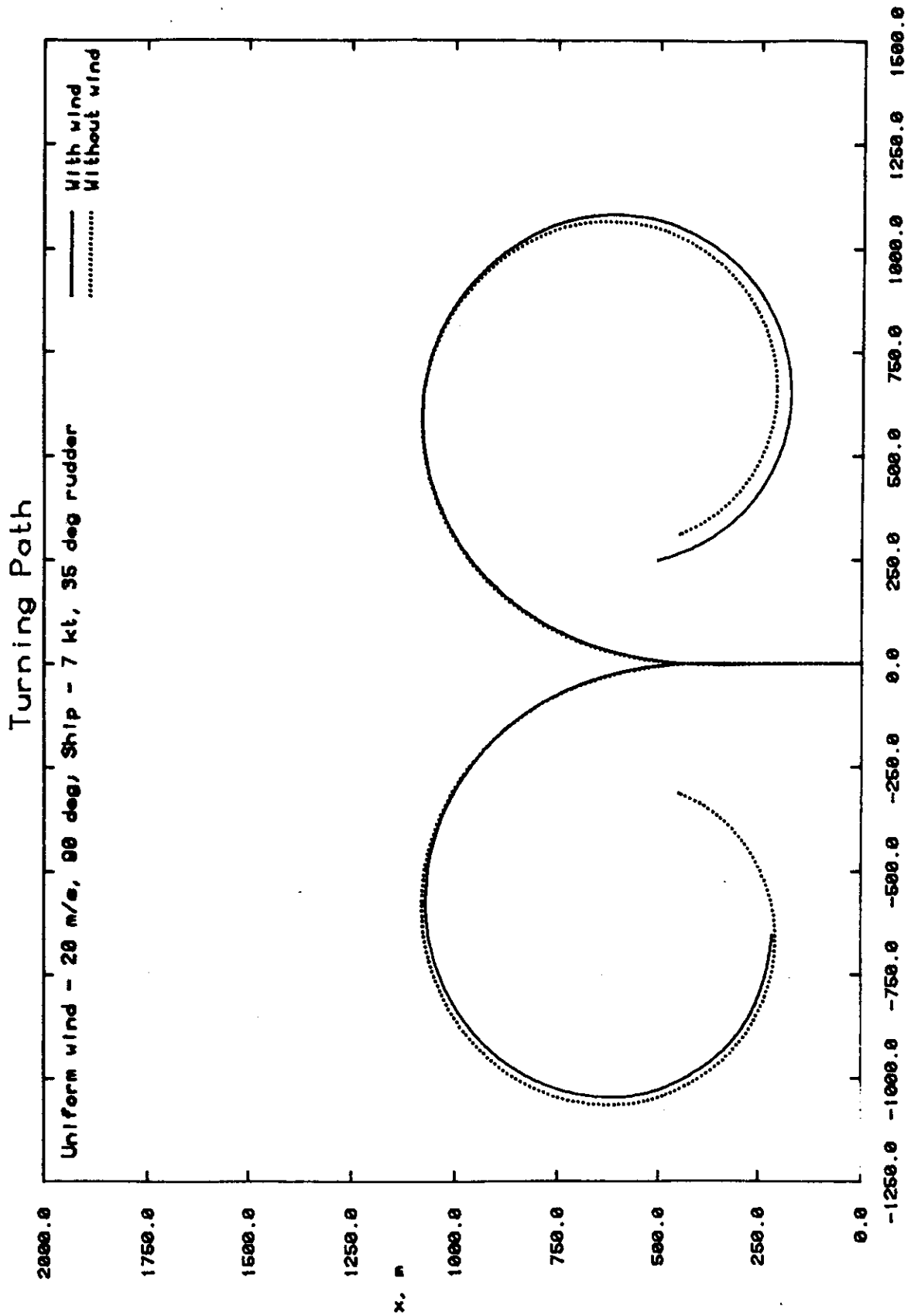

Turning Path - Wind

Figure 4.12

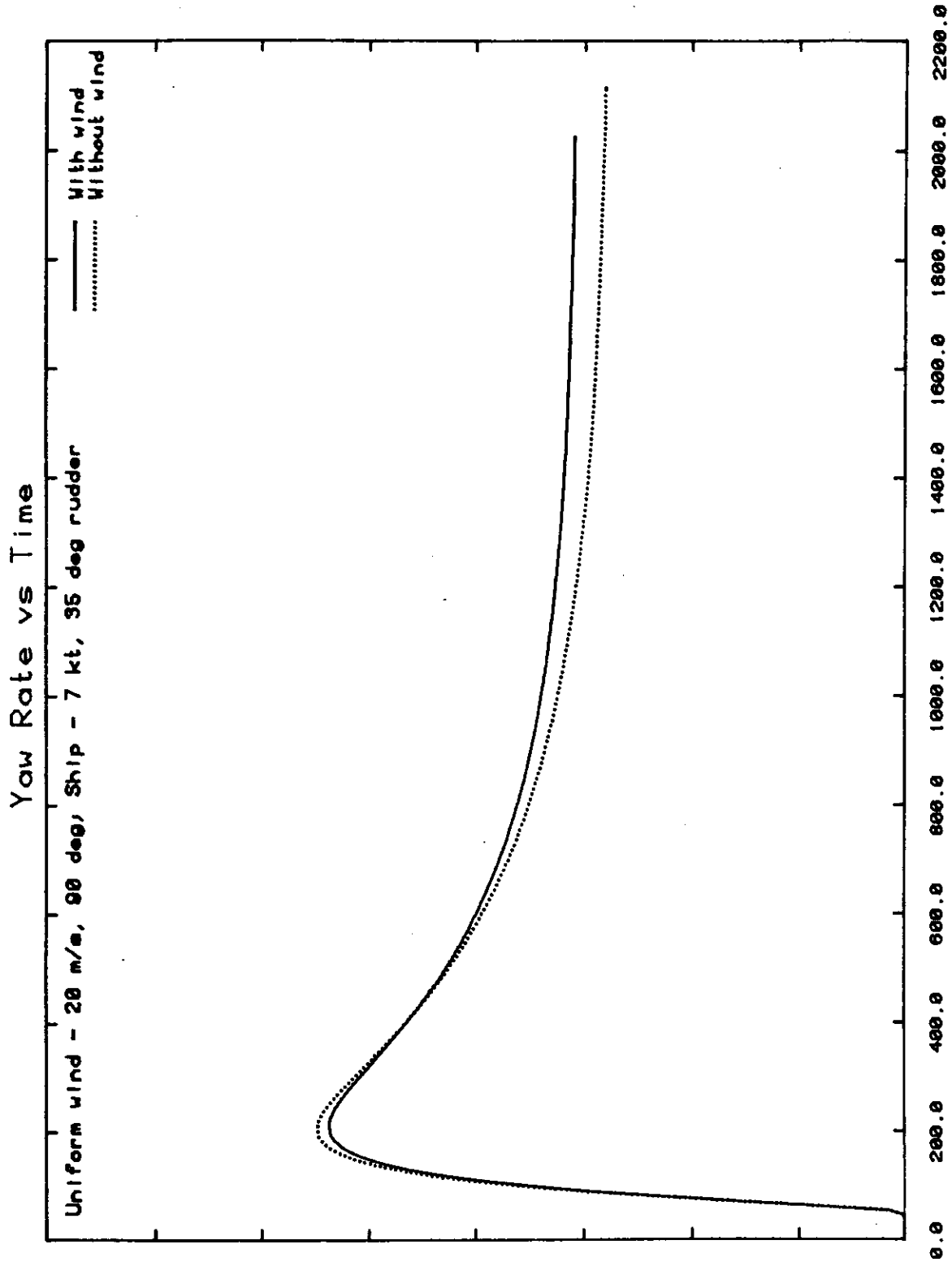

Yaw Rate vs Time - Wind

Figure 4.13

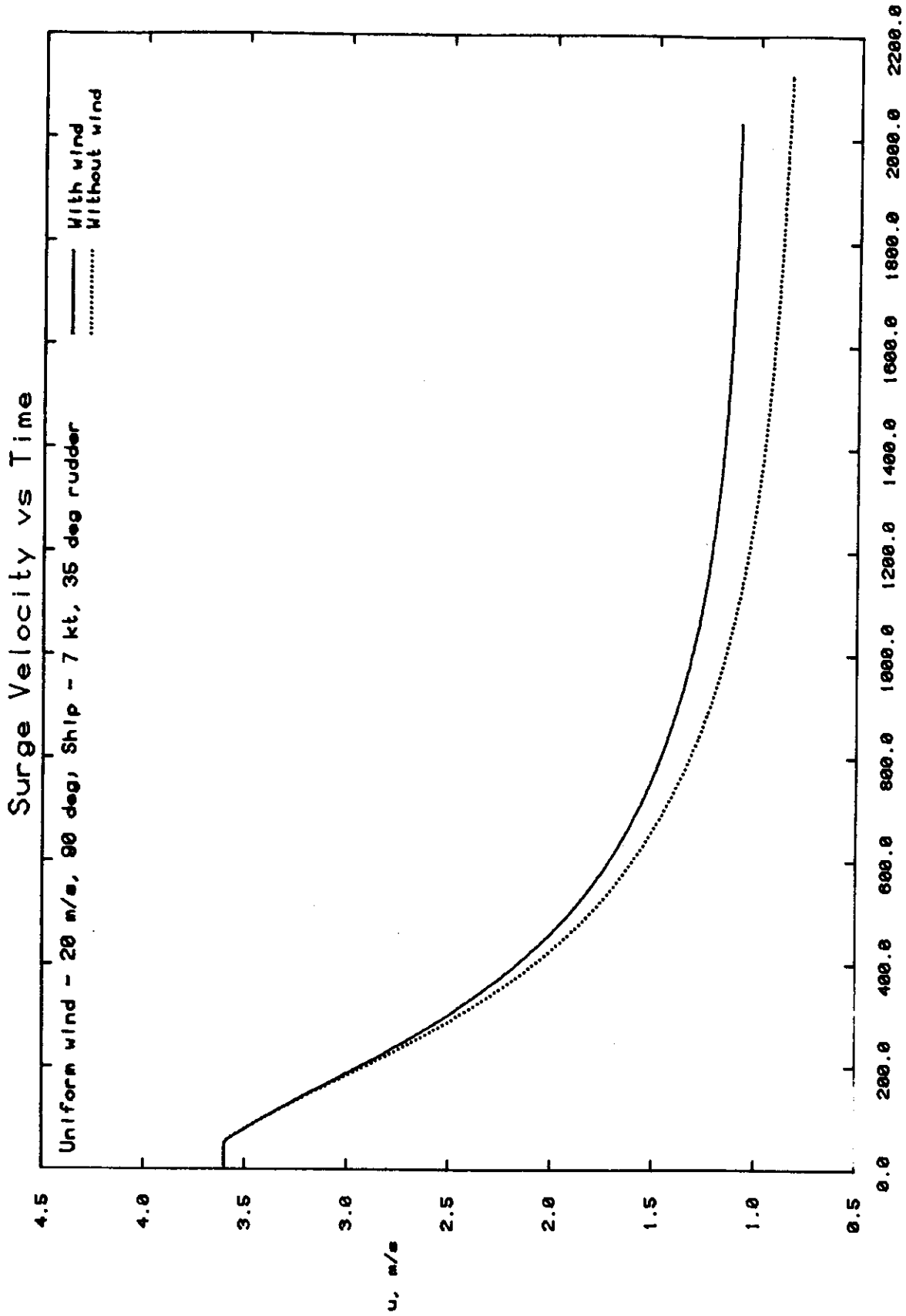

Surge Velocity vs Time - Wind

Figure 4.14

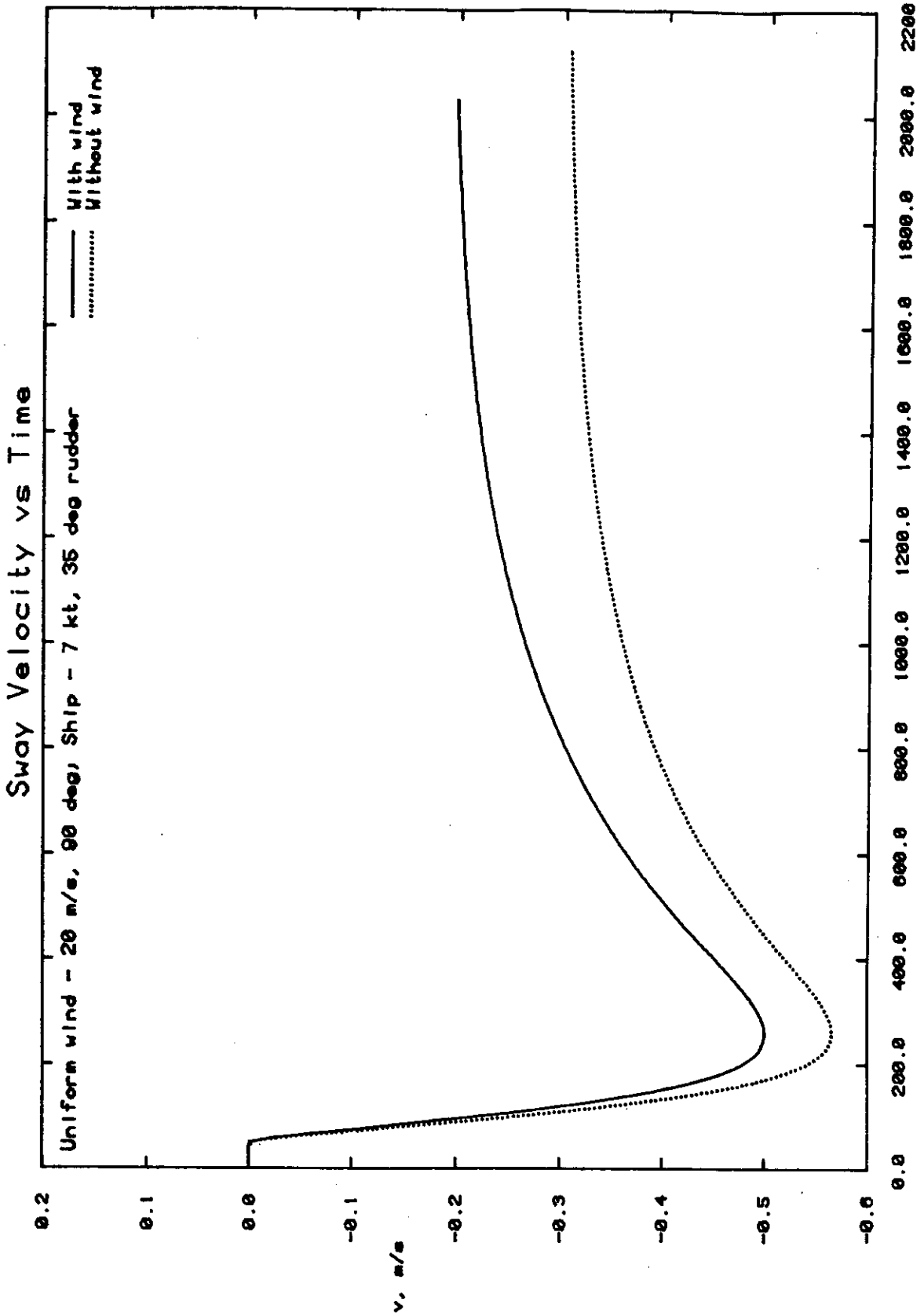

Sway Velocity Vs Time - Wind

Figure 4.15

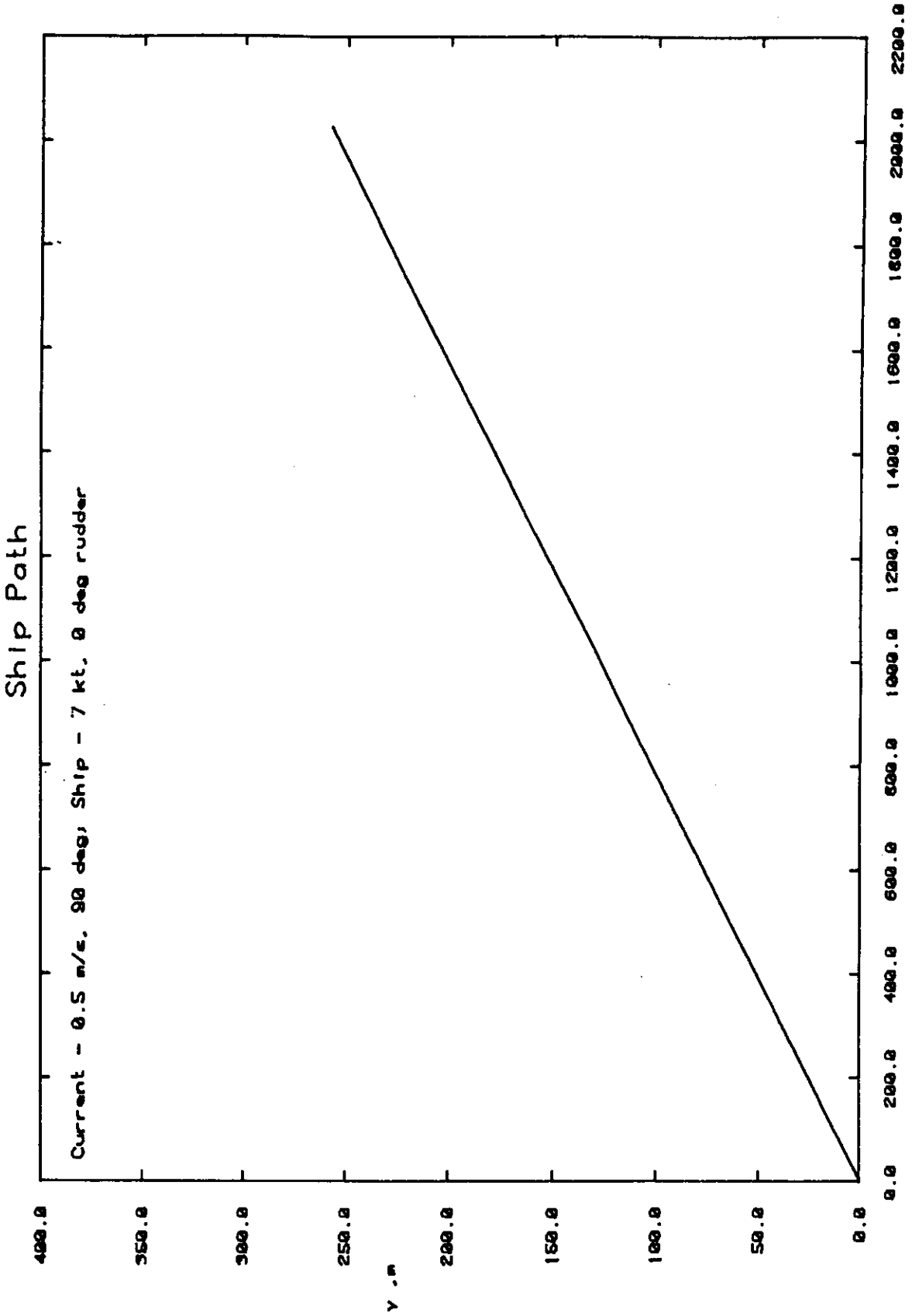

Ship Path ⊥ Current

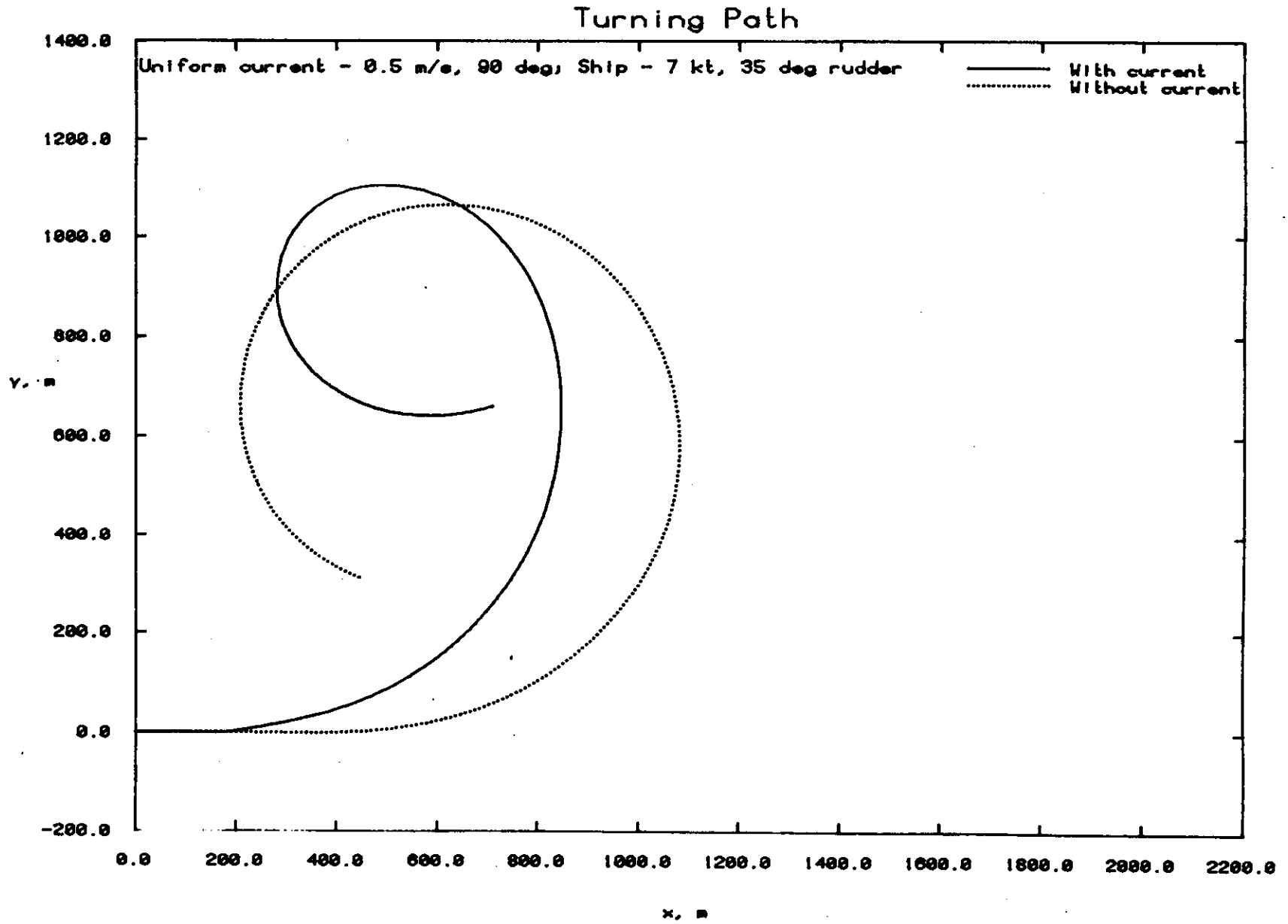

Turning Path - Current

Figure 4.16

Nomenclature

A_B duct cross-sectional area

A_L lateral projected area

A_T transverse projected area

A_R immersed rudder area

A_{SS} lateral projected area of superstructure

A_x maximum cross-sectional area of the hull

a_H ratio of hydrodynamic force, induced on ship hull by rudder action, to rudder force

B breadth of ship

C merit coefficient

C_B block coefficient

C_F channel force coefficient

C_L distance from bow to the lateral-projected-area's centroid

C_M midship section coefficient

C_N yawing moment coefficient

C_p propeller flow-rectification coefficient

C_s ship hull flow-rectification coefficient

C_W waterplane coefficient

C_X fore and aft force coefficient

C_Y lateral force coefficient

D_B impeller diameter

D_p propeller diameter

F_{nh} shallow water Froude number

F_N rudder normal force

h water depth

h_R rudder height

Nomenclature (Continued)

I_{xx}, I_{zz} moment of inertia of ship in roll and yaw respectively

I_{pp} moment of inertia of propeller-shafting system

J_p advance coefficient

K_F body force coefficient

K_M body moment coefficient

K_Q torque coefficient

K_T thrust coefficient

k_{xx} radius of gyration in roll

L waterline length

L_{OA} length overall

L_{pp} length of ship between perpendiculars

M number of distinct groups of masts or kingposts seen in lateral projection

MG metacentric height

m mass of ship

m_x, m_y, m_ψ, m_ϕ added mass (inertia) of ship in surge, sway, yaw, roll respectively

n propeller rpm

n_c command engine rpm

n_{cp} equivalent command propeller rpm

P_p propeller pitch

Q_E torque delivered by power plant

Q_p propeller torque

r yaw rate over ground

r_c yaw rate due to current

r_s yaw rate over water

Nomenclature (Continued)

R_{GEAR} reduction gear ratio

S length of perimeter of lateral projection

SHP engine shaft horsepower

shp thruster shaft horsepower

T draft

t thrust deduction fraction

U ship speed ($\sqrt{u^2+v^2}$)

U_c magnitude of current

U_W relative wind velocity

u ship speed in surge direction

u_c current speed over ground

u_E equilibrium speed corresponds to n_c

u_e ship speed over ground

u_j jet velocity

u_s ship speed over water

V_R effective rudder inflow speed

v ship speed in sway direction

v_c current speed over ground

v_e ship speed over ground

v_s ship speed over water

w_p effective propeller wake fraction

w_{po} effective propeller wake fraction in straight running condition

w_R effective rudder wake fraction

w_{RO} effect rudder wake fraction in straight running condition

x_c location of the center of lateral pressure

Nomenclature (Continued)

x_H point of application of rudder induced interaction force on ship hull

x_M horizontal distance between center of gravity aft of midship

x_P horizontal distance between center of gravity and propeller

x_R horizontal distance between center of gravity and rudder

x_T distance from bow thruster to midship

Y_{CL} off-centerline distance

z_H vertical distance between center of gravity and middle of draft

z_R vertical distance between center of gravity and center of rudder

α depth correction factor

α_R effective rudder inflow angle

β ship drift angle

β_{RR} effective drift angle at rudder

γ flow-rectifying effect

γ_{WIND} relative wind angle

δ rudder angle

θ_c direction of current

λ geometric aspect ratio of the rudder

ρ density of water

ρ_{AIR} density of air

τ trim of ship ($=T_{aft}-T_{fore}$)

Φ roll angle

Ψ heading angle

Δ volume displacement